JOURNAL OF PETROLOGY | VOLUME 51 | NUMBER 3 | PAGES 573–602 | 2010 | doi:10.1093/petrology/egp080

Olivine, and the Origin of Kimberlite

N. T. ARNDT[1]*, M. GUITREAU[2], A.-M. BOULLIER[3], A. LE ROEX[4], A. TOMMASI[5], P. CORDIER[6] AND A. SOBOLEV[7]

[1]LGCA, UNIVERSITÉ JOSEPH FOURIER & CNRS, GRENOBLE 38400, FRANCE

[2]ECOLE NORMALE SUPÉRIEURE DE LYON, LYON 69364, FRANCE

[3]LGIT, UNIVERSITÉ JOSEPH FOURIER & CNRS, GRENOBLE 38400, FRANCE

[4]UNIVERSITY OF CAPE TOWN, CAPE TOWN 7701, SOUTH AFRICA

[5]GÉOSCIENCES MONTPELLIER, UNIVERSITÉ DE MONTPELLIER & CNRS, MONTPELLIER 34095, FRANCE

[6]LSPES, UNIVERSITÉ DE LILLE & CNRS, LILLE 59655, FRANCE

[7]VERNADSKY INSTITUTE, MOSCOW, RUSSIA

RECEIVED JUNE 13, 2009; ACCEPTED NOVEMBER 2, 2009
ADVANCE ACCESS PUBLICATION JANUARY 12, 2010

Two types of olivine occur in kimberlites from Greenland, Canada and southern Africa. The first, xenocrystic olivine, displays several different forms. Most distinctive are 'nodules', a term we use to describe the large (1–5 mm), rounded, single crystals or polycrystalline aggregates that are a common constituent of many kimberlites. Olivine compositions are uniform within single nodules but vary widely from nodule to nodule, from Fo81 to 93. Within many nodules, sub- to euhedral asymmetric tablets have grown within larger anhedral olivine grains. Dislocation structures, particularly in the anhedral grains, demonstrate that this olivine was deformed before being incorporated into the kimberlite magma. Olivine grains in the kimberlite matrix between the nodules have morphologies similar to those of the tablets, suggesting that most matrix olivine grains are parts of disaggregated nodules. We propose that a sub- to euhedral form is not sufficient to identify phenocrysts in kimberlites and provide some criteria, based on morphology, internal deformation and composition, that distinguish phenocrysts from xenocrysts. The second type of olivine is restricted to rims surrounding xenocrystic grains. Only this olivine crystallized from the kimberlite magma. Major and trace element data for the rim olivine are used to calculate the composition of the parental kimberlite liquid, which is found to contain between about 20 and 30% MgO. The bulk compositions of many kimberlites contain higher MgO contents as a result of the presence of xenocrystic olivine. The monomineralic, dunitic, character of the nodules, and the wide range from Fo-rich to Fo-poor olivine compositions, provide major constraints on the origin of the nodules. Dunite is a relatively rare rock in the mantle and where present its olivine is persistently Fo-rich. The dunitic source of the nodules in kimberlites lacked minerals such as pyroxene and an aluminous phase, which make up about half of most mantle-derived rocks. It appears that these minerals were removed from the mantle peridotite that was to become the source of the nodules, and the Fo content of the retained olivine was modified during interaction with CO_2-rich fluids whose arrival at the base of the lithosphere immediately preceded the passage of the kimberlite magmas. Fragments of the resultant dunite were entrained into the kimberlite, where they were retained both as intact nodules and as disaggregated grains in the matrix.

KEY WORDS: *dunite; kimberlite; mantle; olivine; xenolith*

INTRODUCTION

Kimberlite, as illustrated in Figs 1 and 2, is a rock dominated by olivine. Most kimberlites are highly altered and their primary textures are poorly preserved, but rare examples, such as the sample from the Kangamiut region of Greenland shown in Fig. 1, contain about 50% of large fresh olivine grains, which are set in a matrix of finer-grained minerals. Most descriptions of the mineralogy of kimberlite (e.g. Mitchell, 1970, 1986, 1995; Scott-Smith, 1992) have focused on minerals such as

*Corresponding author. Telephone: 33 4 76635931. E-mail: arndt@ujf-grenoble.fr

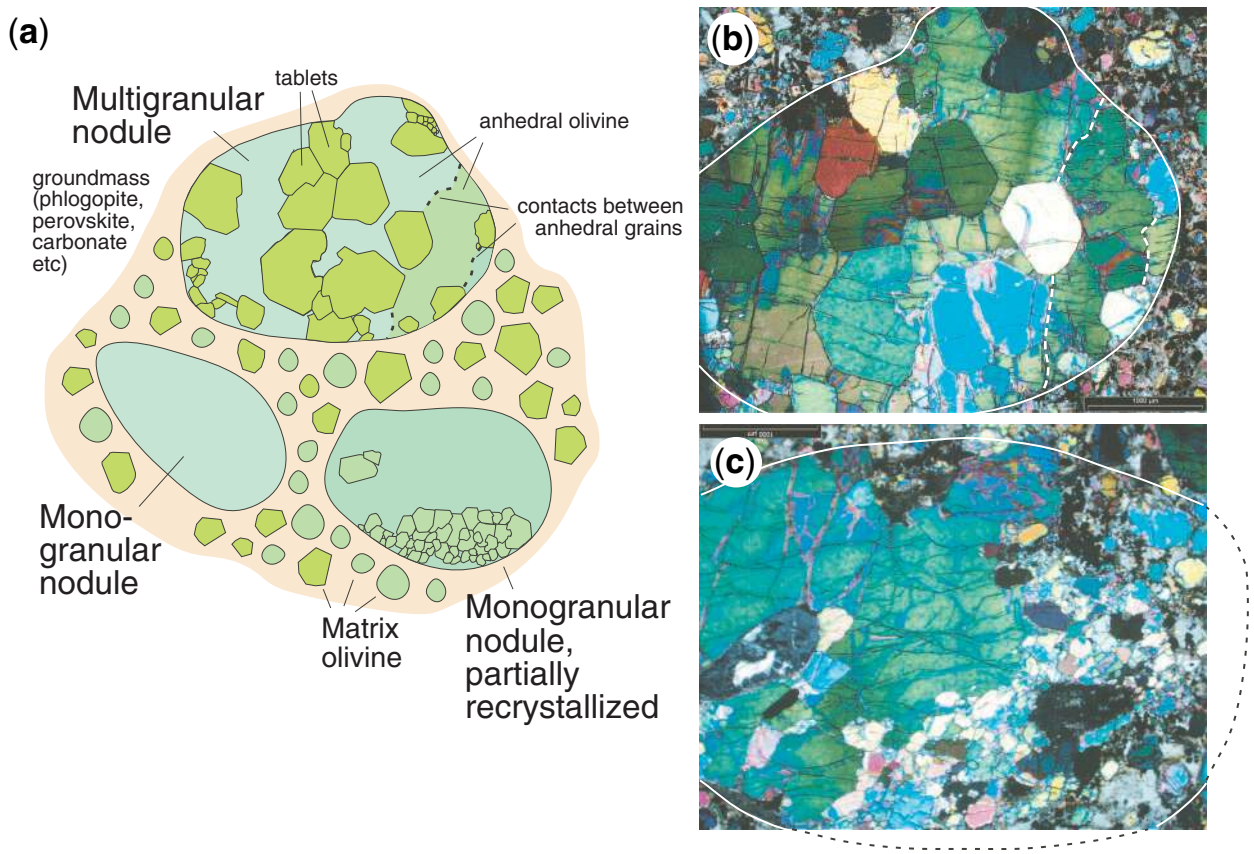

Fig. 1. Sketches and photomicrographs of nodules in sample NCR27 from the Kangamiut region of Greenland. (a) Sketch illustrating the form of olivine in nodules and matrix and presenting the terminology used to describe the various forms of olivine crystals. (b) Photomicrograph of a multigranular nodule with well-developed tablets in sample NCR27. (c) Photomicrograph of another nodule containing fewer tablets and a recrystallized fine-grained portion. Scale bar 1 mm.

Cr-rich diopside, garnet, ilmenite and phlogopite that occur as megacrysts or are present in the groundmass. Numerous detailed studies have emphasized the unusual compositions of these minerals and have shown how they can be used to infer the conditions of kimberlite generation or to act as tracers during diamond exploration. Surprisingly little work has been done, however, on the olivine itself.

In standard texts such as those by Mitchell (1970, 1986, 1995), Clement *et al.* (1983), Moore (1988) and Scott-Smith (1992), a distinction is made between xenocrystic olivine and 'primary' or phenocrystic olivine. The former occurs mainly as 'macrocrysts', a term used to describe large, subangular to rounded, single crystals or crystal aggregates whose habit, undulose extinction and multi-grain character suggest an origin foreign to that of the kimberlite magma. Phenocrystic olivine is said to occur as smaller grains that are identified by a sub- or euhedral habit defined by the presence of planar crystal faces, and by an absence of strain features. The origin of small, rounded, strain-free grains, which also are present in most kimberlites, is ambiguous.

In a recent study, Kamenetsky *et al.* (2008) distinguished two populations of olivine: olivine-I, which occurs as large, rounded grains or subangular fragments, and olivine-II, which occurs as smaller, euhedral to subhedral, flattened tabular grains. Using back-scattered electron images and X-ray element maps, they showed that olivine-II grains were complexly zoned and contained one or more concentric or irregular internal layers that were richer or poorer in Fe and minor elements than the outer margins. They noted that both types contained fluid and melt inclusions, and that both exhibited strain features. These features, together with low and variable water contents, were cited as evidence that olivine-I grains were largely xenocrystic. The origin of olivine-II was more problematic. The compositions of pyroxene and garnet inclusions were used to infer that these grains formed at pressures corresponding to those at the base of the lithosphere. A wide diversity in the size, shape and compositions of the cores of these grains was taken as evidence that they evolved during 'growth, recrystallization, transport, dissolution and regrowth in different mantle–melt and crust–melt

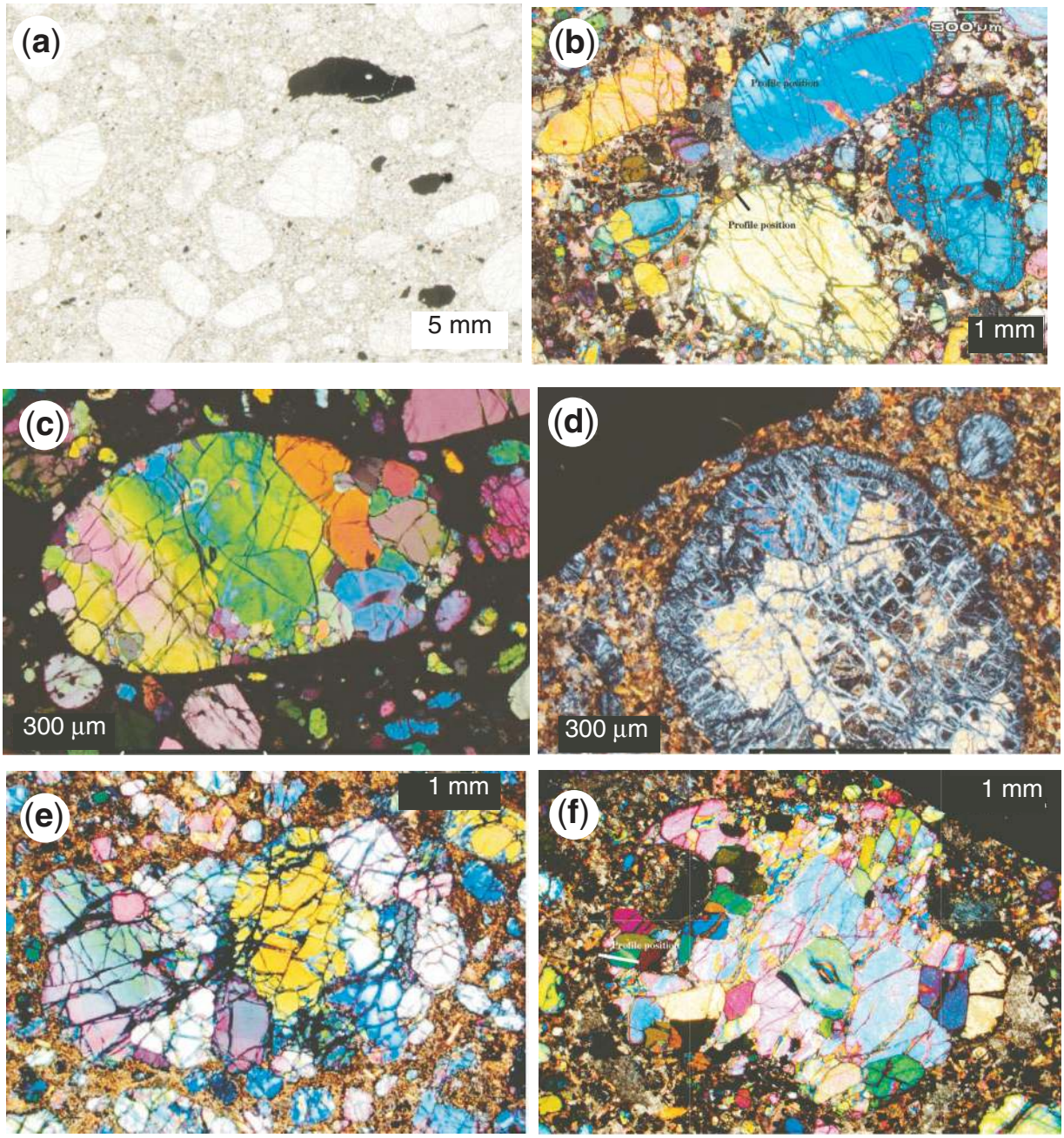

Fig. 2. (a) Scanned thin section, sample NCR27, Kangamiut, Greenland. Rounded to subangular olivine nodules and several ilmenite megacrysts in a groundmass of finer-grained olivine, phlogopite, opaque minerals and carbonate. (b) Nodules in sample NCR27. All are monogranular, except for the small grain in the centre left, which contains a few tablets. (c) Multigranular nodule displaying abundant tablets, sample Plt-7-3 from Botswana. (d) Poorly preserved (serpentinized) multigranular nodule from Ekati, Canada. Tablets are discernible in the upper part of the nodule. (e) Irregular aggregate of olivine grains in sample CRC-7A from the Finch Mine, South Africa. (f) Multigranular nodule in sample NCR27, Kangamiut, Greenland. It should be noted that even though the rounded form is apparent, tablets have been plucked out at the top left and right and the nodule is disaggregating at the lower part.

environments' (Kamenetsky *et al.*, 2008, p. 13). Rims of olivine with uniform major element compositions but variable trace elements were attributed to low-pressure crystallization in the melt that transported the crystals to the surface.

Brett *et al.* (2009) also distinguished two olivine populations; macrocrysts (olivine-I) and euhedral crystals (olivine-II). Both types are overgrown by chemically distinct rims, which they also attributed to growth from the kimberlite melt; they concluded that both types of olivine

grain are xenocrystic. They calculated that the proportion of rim olivine was relatively small, <5%, and concluded that the composition of the kimberlites they studied was dominated by the xenocrystic olivine.

Here we present the results of a detailed investigation of the petrography, mineral structure and chemical compositions of olivine in kimberlites from localities in Greenland, Canada and southern Africa. The work initially focused on two remarkably preserved samples from Greenland but was then extended to other locations. We demonstrate that both the form and composition of the olivine grains in these rocks are distinctive and peculiar to kimberlite, and that these features provide important clues to the origin of the kimberlite magmas themselves. Like Kamenetsky *et al.* (2008) and Brett *et al.* (2009), we conclude that most of the olivine, apart from the thin outer rims, is xenocrystic. However, our analysis of the morphology of these grains and their compositional variations leads us to a different interpretation of the origin of this olivine.

SAMPLES AND ANALYTICAL METHODS

In Table 1 we list all the samples we studied and provide some information about their petrography and location; more detailed descriptions are given in Supplementary Data Table S1 (available for downloading at http://www.petrology.oxfordjournals.org). All samples are hypabyssal kimberlites from dykes or from the root zones of diatremes, and, with few exceptions, they were chosen because their olivine is exceptionally well preserved. Our collection includes two samples from the Kangamiut region of Greenland, 10 samples from the Ekati Mine, one from Snap Lake and five from Somerset Island, all in Canada. Descriptions of the geological setting of these samples have been given by Mitchell (1978), Nowicki *et al.* (2004, 2008), Hutchison (2008) and Francis & Patterson (2008). The seven other samples come from classic localities in southern Africa (see Table 1 and Supplementary Data Table S1). Four of these (Plt-17-03, C-7, K18-348 and Col-1) are macrocrystic Group I kimberlites, whereas the remaining three are macrocrystic Group II phlogopite (CRC-7A, JJG-192) and calcite–phlogopite (JJG-4676) kimberlites. Descriptions of these samples have been given by Smith *et al.* (1985), Mitchell (1986, 1995) and Becker & le Roex (2006).

Olivine compositions were determined semi-quantitatively using an EAGLE III micro X-ray fluorescence spectrometer at the University Joseph Fourier in Grenoble, and quantitatively using a Cameca SX-50 electron microprobe in Grenoble and a JEOL Superprobe JXA-8200 electron microprobe at the Max Planck Institute for Chemistry, in Mainz, Germany. The analytical conditions for the Cameca Sx-50 micropobe were 20 kV accelerating voltage and 20 nA primary electron beam current, with 60 s peak and 30 s background counting times. We used JXA-8200 microprobe for extra precise olivine analysis at 300 nA beam current, 20 kV accelerating voltage and long counting times (see Sobolev *et al.*, 2007.

Major element abundances in the samples from Kangamiut and the Ekati Mine were determined at the Service d'Analyse des Roches et des Minéraux (SARM) in Nancy using techniques described on their website http://helium.crpg.cnrs-nancy.fr/SARM/indexanglais.html. Trace elements were analysed by inductively coupled plasma mass spectrometry (ICP-MS) at the University Joseph Fourier in Grenoble. Analytical procedures, estimated errors, values for reference samples, and other documentation have been given by Marini *et al.* (2005) Analyses are listed in Supplementary Data Table S2. The compositions of the other samples have been reported by Becker & le Roex (2006) and Francis & Patterson (2008).

Dislocation microstructures in olivine were studied on thin sections that had been prepared using the technique described by Kohlstedt *et al.* (1976). A rock section was heated at 900°C for 1 h in air and a polished thin section was then made from this oxidized section. During the heating, oxygen diffuses along dislocation lines, which then become visible under a petrographic microscope. These thin sections were then studied under an LEO STEREOSCAN 440 scanning electron microscope (SEM) at CISM (Savoie University) in backscattered electron mode under conditions similar to those proposed by Karato (1987). More detailed studies were conducted with a Philips CM 30 (300 kV) transmission electron microscope (TEM) at LSPES (Lille 1 University) on samples thinned by ion-beam milling.

Preferred orientations of olivine crystals were determined by indexation of electron-backscattered diffraction patterns using facilities at Geosciences Montpellier. Patterns were generated by interaction of a vertical incident electron beam with a carefully polished thin section tilted at 70° in a JEOL JSM 5600 SEM. The diffraction pattern was projected onto a phosphor screen and recorded by a digital charge coupled device (CCD) camera. The image was then processed and indexed in terms of crystal orientation using the CHANNEL5 software from HKL–Oxford Instruments.

PETROGRAPHY

The proportions and types of minerals are summarized in Table 1. All the samples contain the usual suite of kimberlite minerals: olivine, ilmenite, phlogopite and garnet as macrocrysts and olivine, phlogopite, Fe–Ti oxides, perovskite, monticellite, apatite and carbonate in the matrix. Some also contain orthopyroxene, garnet and ilmenite megacrysts. The habits and compositions of all these

Table 1: Summary information about kimberlite samples

Location:	Kangamiut, Greenland	Kangamiut, Greenland	AK6, Botswana	Wesselton, S. Africa	Benfontein, S. Africa	Colville, S. Africa	Finsch, S. Africa	Newland, S. Africa	Bellsbank, S. Africa
Group:	I	I	I	I	I	I	II	II	II
Sample:	NCR 27	NCR 29	Plt-17-03	C-7	K18-348	Col-1	CRC-7A	JJG-192	JJG-4676
Texture	Abundant complex nodules	Aphanitic	Abundant complex nodules	Abundant mono-granular nodules	Aphanitic	Sparse mono-granular nodules	Abundant mono-granular nodules	Abundant mono-granular nodules	Sparse mono-granular nodules
Proportion and morphology of olivine:									
Nodules	~40% of mono- and multigranular nodules, up to 9 mm × 5 mm	<5% small mono-granular nodules	Subangular to rounded mono- and multi- granular nodules; many containing tablets or recrystallized zones	Elongate, well-rounded mono-granular nodules (1–2 contain sparse tablets)	Absent	Sparse angular monogranular nodules	Monogranular; some aggregates of anhedral grains and a few poorly developed tablets	Large angular, sub-rounded mono-granular nodules	Sparse large sub-angular to well-rounded mono-granular nodules; no strain features
Matrix	20% small, rounded or rarely euhedral asymmetric grains	20% small, euhedral and rounded grains of olivine	20% abundant angular fragments, rare rounded or subhedral grains	20%; 1 mm to <0·1 mm; equant rounded, rarely Subhedral	40% euhedral to rounded symmetrical grains; zoning and undulose extinction	20%; equant to elongate, subhedral to well rounded	Angular to rounded fragments, rounded and subhedral grains are uncommon	Sparse small sub-rounded grains	35%; fragment-shaped to elongate rounded
Fo contents:									
Nodules	85·3–91·5		82·4–92–7	86·7–94·6			90·6–93·5		
Tablets	88·2–91·3		87·4–88·2	87·3			90·9–92·8		
Matrix	87·0–91·7	81·7–91·5	83·3–91·8		86·7–93·5		91·3–93·2		
Rims	84·4–90·9	84·9–90·2	86·4–90·5	86·4–93·4	86·7–90·6		90·1–93·6		
Macrocrysts	ilmenite, opx	none	ilmenite, opx (?)			garnet		garnet	
Matrix minerals: extent of alteration (% of olivine preserved)	Very fresh (98%)	Very fresh (95%)	Very fresh (99%)	Minor serpentinization (90%)	Moderate serpentinization (85%)	Moderate serpentinization (50%)	Minor serpentinization (95%)	Moderate serpentinization (60%)	Very fresh (99%)
Remarks	Remarkable, complex well-preserved nodules	Excellent preservation of matrix olivines	Remarkable, complex, well- preserved nodules				Nodules cut by numerous fractures		

(continued)

Table 1: Continued

Location:	Ekati Mine, Canada									
Group:	I									
Sample:	151·6m	162·2mm	372·5m	372·8m	42·2m	45·5m	109·2m	124·0m	127·0m	140·7m
Olivine:										
Nodules	Abundant large (to 5 mm) subangular to rounded nodules	Abundant large (to 5 mm) subangular to rounded nodules	Abundant large nodules	Aphanitic	Abundant large (to 8 mm) subangular to rounded nodules	Well-rounded small (<3 mm) nodules	Sparse small (to 4 mm) subangular to rounded nodules	Abundant large (to 5 mm) subangular to rounded nodules	Sparse small (to 4 mm) subangular to rounded nodules	Sparse large (to 5 mm) subangular to rounded nodules
Matrix	Up to 40% completely altered grains	Small completely altered grains (0·03–0·4 mm)	Small completely serpentinized grains	Small completely serpentinized grains	25% of rounded to subhedral serpentinized grains	Small completely serpentinized grains	Small completely serpentinized grains	Small completely serpentinized grains	Small completely serpentinized grains	Small, rounded completely serpentinized Grains
Macrocrysts		ilmenite, opx						opx	ilmenite	
Extent of alteration	Complete	Intense (5%)	Complete, recrystallized	Complete	Moderate (5–50%)	Complete	Complete	Complete	Complete	Complete

Location:	Somerset Island, Canada					Snap Lake, Canada
Group:	I					I
Sample:	NK1-K4	NK2-K2	NK3-K1	NK3-K2	NK3-K5	SN-1
Olivine:						
Nodules	Sparse, rounded, monogranular	Well-rounded, monogranular; no strain features	Elongate to equant well-rounded monogranular; a few tablets	Sparse, rounded monogranular	Sparse, rounded monogranular	Abundant large (to 5 mm) subangular to rounded Nodules
Matrix	Small rounded to angular with a few subhedral grains	35% equant to elongate, euhedral to rounded grains	Prismatic euhedral to well-rounded; many angular fragments	Euhedral to rounded grains	Euhedral toyrounded grains	
Macrocryst		ilmenite	garnet	garnet, ilmenite, opx(?)	Opx	Ilmenite
Extent of alteration	Minor serp (90%)*	Very fresh (99%)	Minor serp (90%)	Moderate serp (80%)	Moderate serp (50%)	Complete

*Per cent of preserved olivine.

minerals have been described in detail in numerous publications and we will not discuss them further. Our focus is on the olivine.

NCR27 and NCR29 from the Kangamiut region, Greenland

The remarkable character of the olivine grains in these samples has been described briefly by Arndt *et al.* (2006). Olivine is the dominant component of sample NCR27, making up 50% of typical thin sections. It occurs in several distinct forms, of which the most striking are large subangular to rounded grains up to 5 mm × 9 mm that constitute about 40% of the sample (Figs 1 and 2). Normal practice, as exemplified in papers by Mitchell (1986) or Scott-Smith (1992), would be to refer to these objects as 'macrocrysts'; however, this term fails to convey their multigranular nature and morphological complexity. Arndt *et al.* (2006) referred to them as 'nodules' and although we are not entirely happy with the term, we are unable to find an alternative that adequately describes their complex nature. An alternative would be to call them RMMOAs (for Rounded Mono- or Multigranular Olivine Aggregates) but we prefer not to add another acronym to an already overcrowded literature.

In typical thin sections of sample NCR27, about half the nodules consist of single grains, referred to as monogranular nodules in Fig. 1a. The remainder have a wide variety of morphologies and internal structures. The multigranular nodule shown in Fig. 1b is composed of subhedral olivine tablets, about 0·3–1 mm across, which are embedded in anhedral olivine grains with slightly larger but more variable grain size. The form of the tablets is distinctive in that 3–5 crystal faces of each grain are well developed and meet at solid angles between 120 and 140°, whereas the remaining faces are irregular or rounded (Fig. 1b). The average solid angle measured between 812 crystal faces of tablets in four nodules is 140°, as shown in the histogram (Fig. 3c and d). Another feature of the tablets is the variable length of the crystal faces, which makes the tablets asymmetric. The shape of these grains is subtly different from that of typical olivine phenocrysts, as illustrated by the olivine grain in a mid-ocean basalt in Fig. 4f. Although this grain is also asymmetric, opposing faces have equal lengths, unlike faces of the tablets, which may all have different lengths.

The anhedral olivine that encloses the tablets commonly has undulose extinction and multiple subgrain boundaries, as a result of the organization of dislocations within the crystals, and is cut by numerous fractures. Other nodules in sample NCR27 are composed of large anhedral olivine crystals cut by zones consisting of a mosaic of smaller grains whose texture resembles that of a recrystallized mylonite (Fig. 1a and c). In the nodule shown in Fig. 1a and b, a slight difference in polarization tints indicates that the anhedral olivine comprises at least three separate grains. Below, we will use these aspects of the morphology of the tablets to distinguish between various types of olivine grains in kimberlites.

About half of the nodules consist of single grains; for these the term macrocryst is entirely adequate, but because they form part of the population that includes the more complex objects described above we prefer to call them monogranular nodules. The outlines of the nodules are moderately to extremely well rounded, giving many of them an elliptical or peanut-like shape. The outer rounded margin cuts indiscriminately across tablets and anhedral olivine grains in multigranular nodules, indicating that the rounding took place after the tablets had formed.

Olivine also occurs as smaller grains in the matrix between the nodules. At this point we must raise another problem of terminology: we have to distinguish between the anhedral olivine that encloses the tablets within the nodules and the olivine grains that are present in the groundmass between the nodules. For both forms the term 'matrix olivine' would be appropriate, but because the nature and origin of these grains is very different we avoid possible confusion by using the term 'anhedral olivine' for the material between tablets within the nodules and 'matrix olivine' for the smaller grains between the nodules. The use of these terms is illustrated in Fig. 1a.

Olivine in the matrix has a serial variation in size, from about 1 mm to less than 0·1 mm. The habit ranges from subhedral (almost all grains show some degree of rounding) to elliptical. Many grains are similar in size and morphology to the tablets in the nodules—they retain, for example, the near-140° crystal faces and the dissimilar lengths of crystal faces. Below, we will develop the hypothesis that many or most of them are parts of disaggregated nodules. These grains are embedded in a groundmass in which we have identified phlogopite, carbonates (calcite and dolomite), iron oxides, apatite and perovskite as well as serpentine and chlorite after olivine.

Other minerals are present as discrete macrocrysts. Ilmenite is the most common, occurring as large subrounded grains or aggregates of grains (Fig. 2a); however, orthopyroxene and garnet are also present. A notable feature of the latter is that they are surrounded by reaction rims and are clearly out of equilibrium with the kimberlitic magma. Figure 4e shows a rare grain of orthopyroxene in a multigranular olivine nodule. The rounded outline of the orthopyroxene grain contrasts with the euhedral forms of the olivine tablets and matrix grains.

Our only other sample from the Kangamiut region, NCR29, contains less than 5% of small nodules in a matrix with a mineralogy and texture similar to that of sample NCR27. The matrix olivine grains range in size

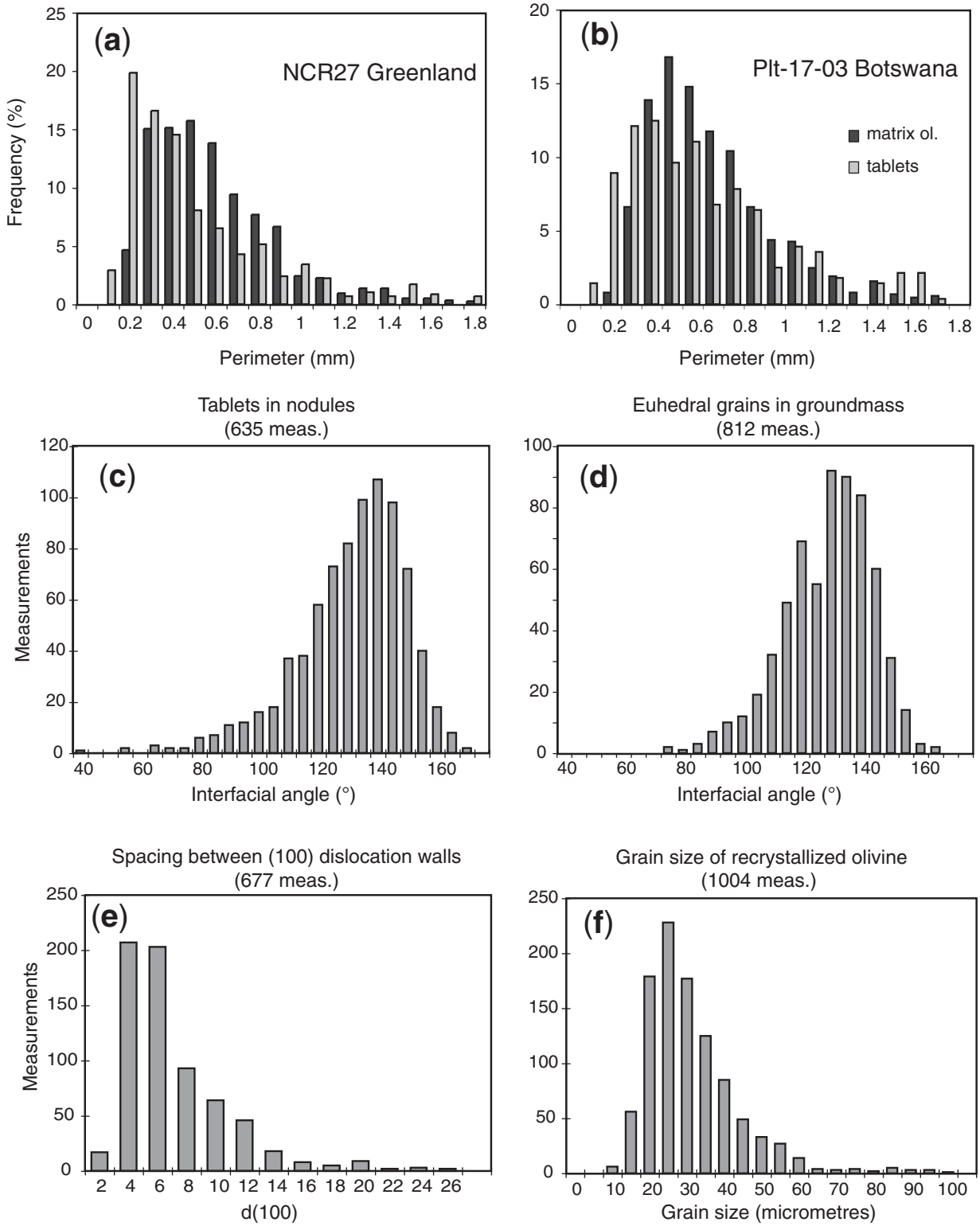

Fig. 3. Histograms of olivine sizes and forms. (a, b) Comparison between the perimeters of tablets in multigranular nodules and those of matrix grains; (c, d) comparison of interfacial angles of tablets and matrix grains in sample NCR27; (e) distance between dislocation walls in anhedral olivine grains in sample NCR27; (f) grain size of dynamically recrystallized olivine in nodules of sample NCR27.

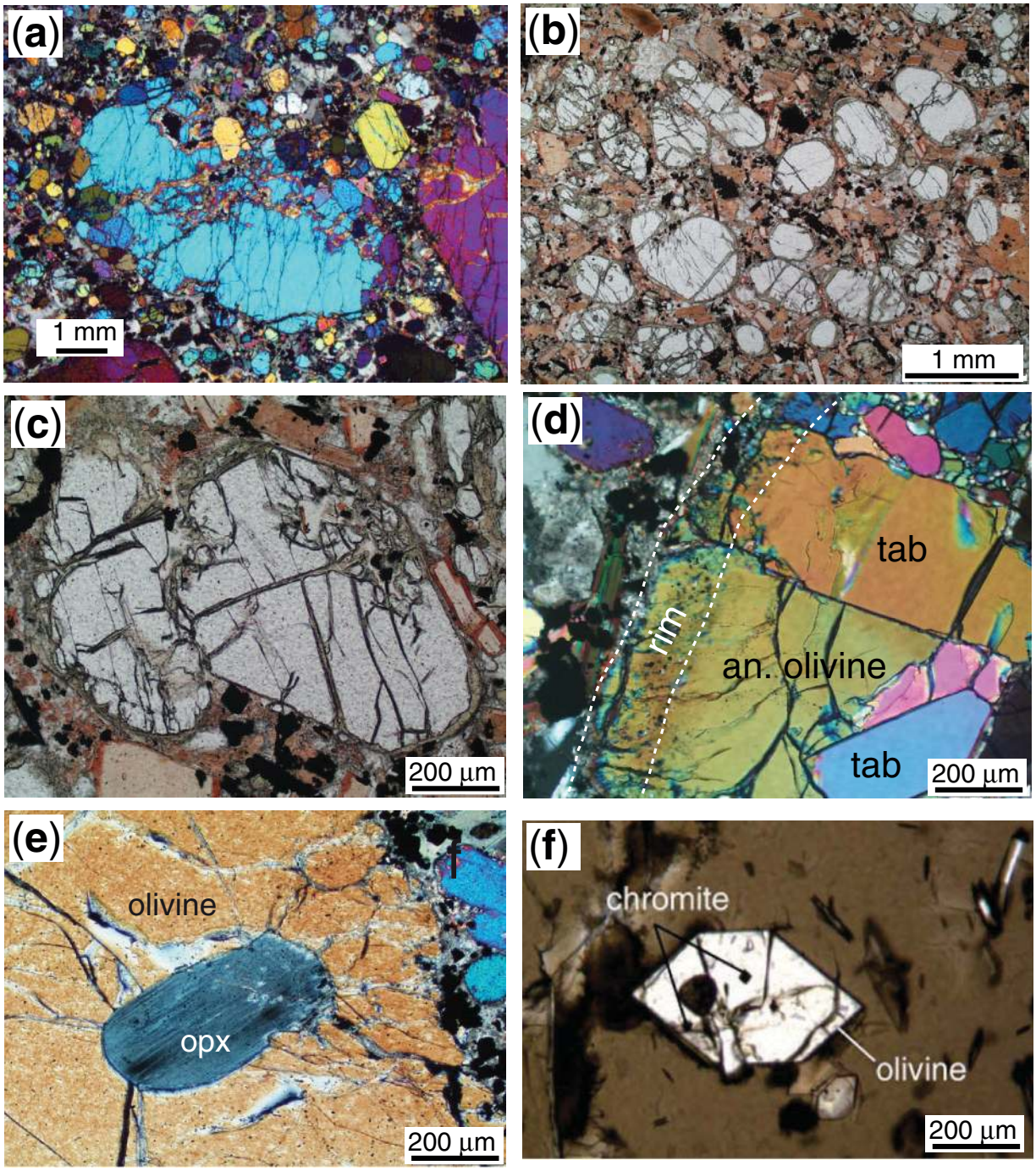

Fig. 4. Photomicrographs of kimberlites. (a) Olivine nodules in sample NCR27 in the process of disaggregating into detached tablets and anhedral grains; (b) rounded to subhedral olivine grains in sample NCR29; (c) two subhedral asymmetric grains with an irregular mutual contact in sample NCR29; (d) an asymmetrical subrounded grain in sample NCR29; (e) a rare example of an orthopyroxene grain in a olivine nodule of sample NCR27 (note the rounded margins); (f) symmetrical olivine grains in a basaltic pillow rim.

from about 0·5 to 1 mm and their form varies from well rounded to euhedral. The nodules retain the same distinctive asymmetric morphology as the tablets in the nodules of sample NCR27. Figure 4a–c shows typical examples that display near−140° interfacial angles, five crystal faces of dissimilar length, and in some cases an irregular sixth face.

No macrocrysts of orthopyroxene or garnet were observed in this sample. Phlogopite is abundant (~40%) and occurs both as a phenocryst phase and as anhedral

grains in the groundmass. The phlogopite phenocrysts are tabular, up to 0·1 mm thick and 0·4 mm long, and always have rounded outlines. Most are strongly zoned, with strongly pleochroic mantles surrounding weakly pleochroic cores. Other minerals identified in the groundmass are carbonate, iron oxides, apatite and perovskite.

Kimberlites from other regions

Although no other sample in our collection contains abundant, spectacular olivine nodules like those of sample NCR27, similar features are also found in kimberlites from many other areas. All eight samples from the Ekati mine in Canada contain large rounded grains of olivine that resemble those of sample NCR27, both in terms of their size and their external shape. In addition, although most of these grains are so serpentinized that their internal features have been lost, some samples retain sufficient unaltered olivine that a multigranular, tablet-and-matrix texture like that in NCR27 can be discerned (Fig. 2d). These samples are probably very similar to those from the Kangamiut region. Similarly, a sample from Snap Lake, also in Canada, contains abundant nodule-shaped and nodule-sized grains; however, these are so thoroughly serpentinized and recrystallized that all internal structure has been lost.

A sample of Group I kimberlite from Botswana (Plt-17-03) contains well-preserved nodules that are identical to those from the Kangamiut region in all important respects, as in the example illustrated in Fig. 2c. This nodule contains subhedral olivine tablets of various sizes embedded in anhedral olivine with undulose extinction, both types within a single peanut-shaped nodule with a well-rounded outline. Sample C7 from the Wesselton Mine contains a few nodules with isolated olivine tablets and most of our other South African samples contain abundant monogranular nodules. Sample CRC-7a from the Finsch Mine in South Africa contains aggregates of multiple olivine grains with irregular to well-rounded outlines (Fig. 2e). This occurrence is significant because this sample is a Group II kimberlite unlike the others described above, which are all of Group I. This indicates that olivine nodules are found in both types of kimberlite. Samples from Somerset Island contain irregular olivine aggregates and monogranular nodules of various sizes.

In some other samples, K18-348 from Benfontein, South Africa being the best example, the form of the olivine crystals is subtly different. In this sample the majority of the grains are moderately rounded; however, those grains that preserve crystal faces whose solid interfacial angles cluster around two values, 44° and 80°, are symmetrical about one or more axes. They commonly contain inclusions of small, equant, euhedral to rounded grains of chromite. The outer form of these crystals closely resembles that of phenocrysts in picritic lavas (Fig. 4f), but they also display abundant strain features, such as undulose extinction and dislocation planes, and at least their internal portions are xenocrystic.

DEFORMATION FEATURES

Microstructures

The anhedral olivine within the nodules displays abundant evidence for intracrystalline deformation, including undulose extinction (Fig. 1b) and well-developed subgrain boundaries, recrystallization at grain boundaries and complete recrystallization leading to a mosaic texture in parts of the nodules (Fig. 1c). When two or more large deformed olivine grains are present in a nodule, their grain boundaries are irregular, one grain locally bulging into the other, or the contact is lined by small recrystallized grains. In marked contrast to the anhedral grains, the tablets exhibit a homogeneous extinction; they are undeformed and they cut indiscriminately across the subgrain boundaries of the anhedral crystals (Fig. 1b). These features are very similar to those described in peridotite xenoliths in kimberlites by Boullier & Nicolas (1975), Guéguen (1977), Green & Guéguen (1983) and Drury & Van Roermund (1989).

Electron backscatter diffraction measurements on multigranular nodules in sample NCR27 allowed us to investigate the orientation relations between deformed anhedral olivine, recrystallized domains, and tablets. Figure 5 is a crystallographic orientation map of a multi-granular nodule composed of a large anhedral olivine crystal with well-developed dislocation walls, surrounded by recrystallized grains and some tablets. Comparison of the orientation maps (Fig. 5a and b) and stereoplots (Fig. 5c and d) confirms that subgrain walls are dominantly (100) tilt walls, indicating that the main glide direction is [100]. Misorientation across dislocation walls may be up to 5°. Analysis of the misorientation within the anhedral olivine crystal (Fig. 5c) shows that [001] and [010] are the dominant rotation axes for the (100) dislocation walls, indicating that they are mainly formed by dislocations of the [100](010) and [100] (001) glide systems. Tablets show a strong misorientation relative to the deformed host olivine crystal (Fig. 5d). They either show an orientation indicating a common axis and an important rotation of the other two axes, or they do not share any crystallographic axis with the host anhedral olivine (compare Fig. 5c and d). In contrast, analysis of a partially recrystallized monogranular nodule in sample NCR27 shows that, although the orientations of recrystallized olivine crystals are highly dispersed, there is a clear orientation inheritance between the host deformed anhedral olivine and dynamically recrystallized olivine grains, as commonly observed in deformed mantle peridotites (Poirier & Nicolas, 1975).

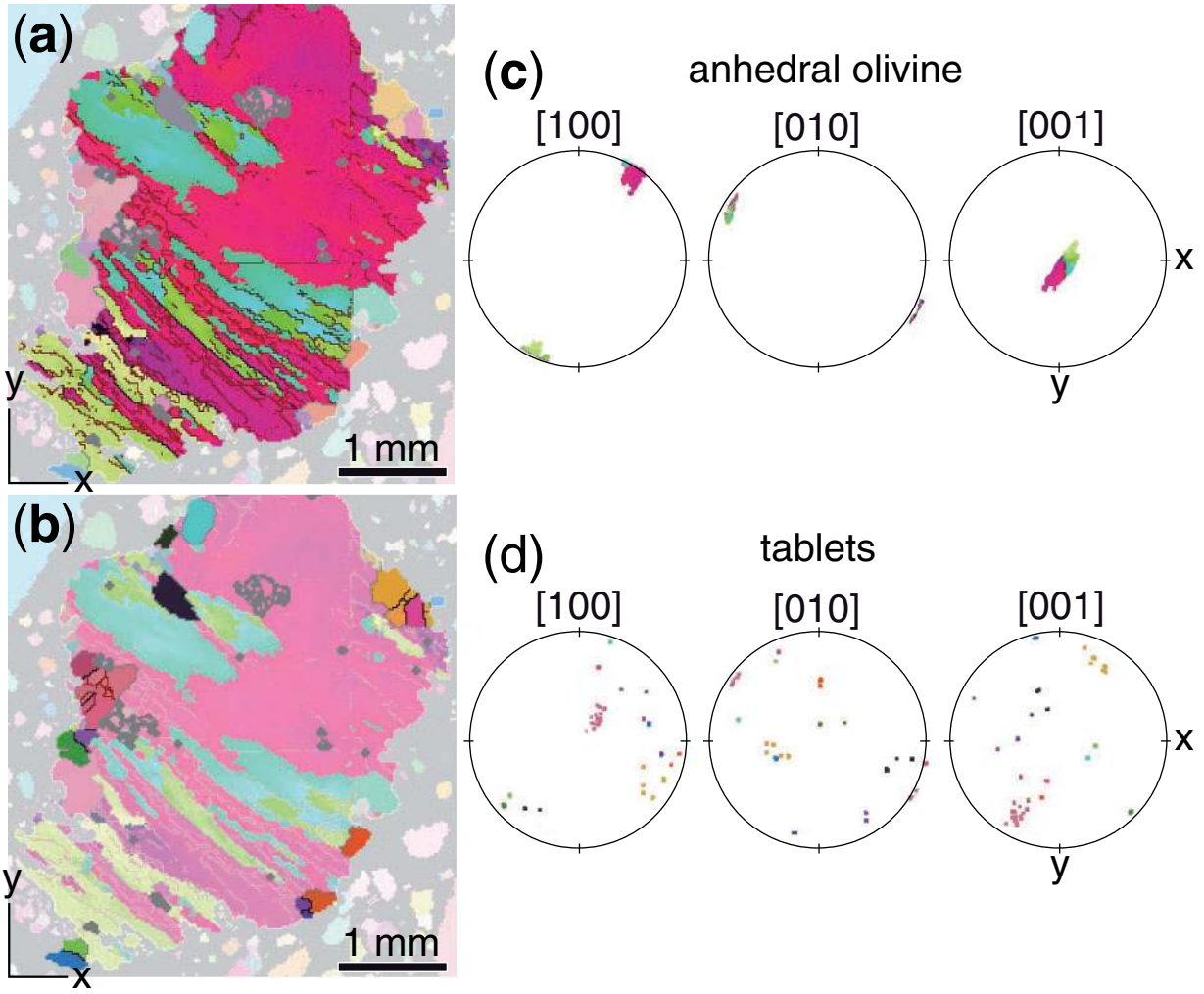

Fig. 5. Crystallgraphic orientation of olivine in a multigranular nodule from NCR27 as measured by electron-backscattered diffraction. (a) Orientation map of the deformed anhedral olivine. (b) Orientation map of the tablets. (c) Stereogram showing the orientation of crystallographic axes in the anhedral olivine [lower hemisphere, colours as in (a)]. (d) Stereogram showing the orientation of crystallographic axes in the tablets [lower hemisphere, colours as in (b)].

Dislocation microstructures

We studied the dislocation microstructures in thin sections prepared using the decoration technique of Kohlstedt *et al.* (1976). Although the oxidation is heterogeneous as a result of fracturing of the grains, the anhedral olivine are generally more highly oxidized than the tablets (Fig. 6a), indicating that they have a higher dislocation density.

Dislocation structures in some of these anhedral olivines take the form of open and closed loops with which are associated short straight segments (Fig. 6c). The undulose extinction of the deformed anhedral olivines is associated with closely spaced subgrain boundaries that have two crystallographic orientations: (100) is the major one (Fig. 6d) and (00l) the minor. The distance between (100) dislocation walls is 5 μm on average (Fig. 3e), but varies between 3 and 10 μm. The average grain-size of dynamically recrystallized olivine was also measured. To avoid grains formed by grain-boundary migration, we measured only the more oxidized grains; that is, those grains displaying a high dislocation density (Fig. 6b). As shown in Fig. 3f, their average size is around 25 μm.

In addition to being far less oxidized than the other olivine grains, some olivine tablets (Fig. 6a and e) show sparse dislocations normal to the crystal boundaries (Fig. 6e). The cores of matrix olivines display dislocation microstructures similar to those observed in the anhedral olivine (compare Fig. 6f with Fig. 6c) and their outer rims are generally characterized by peculiar and numerous straight dislocations oriented at a high angle to the surface of the grain (Fig. 6f).

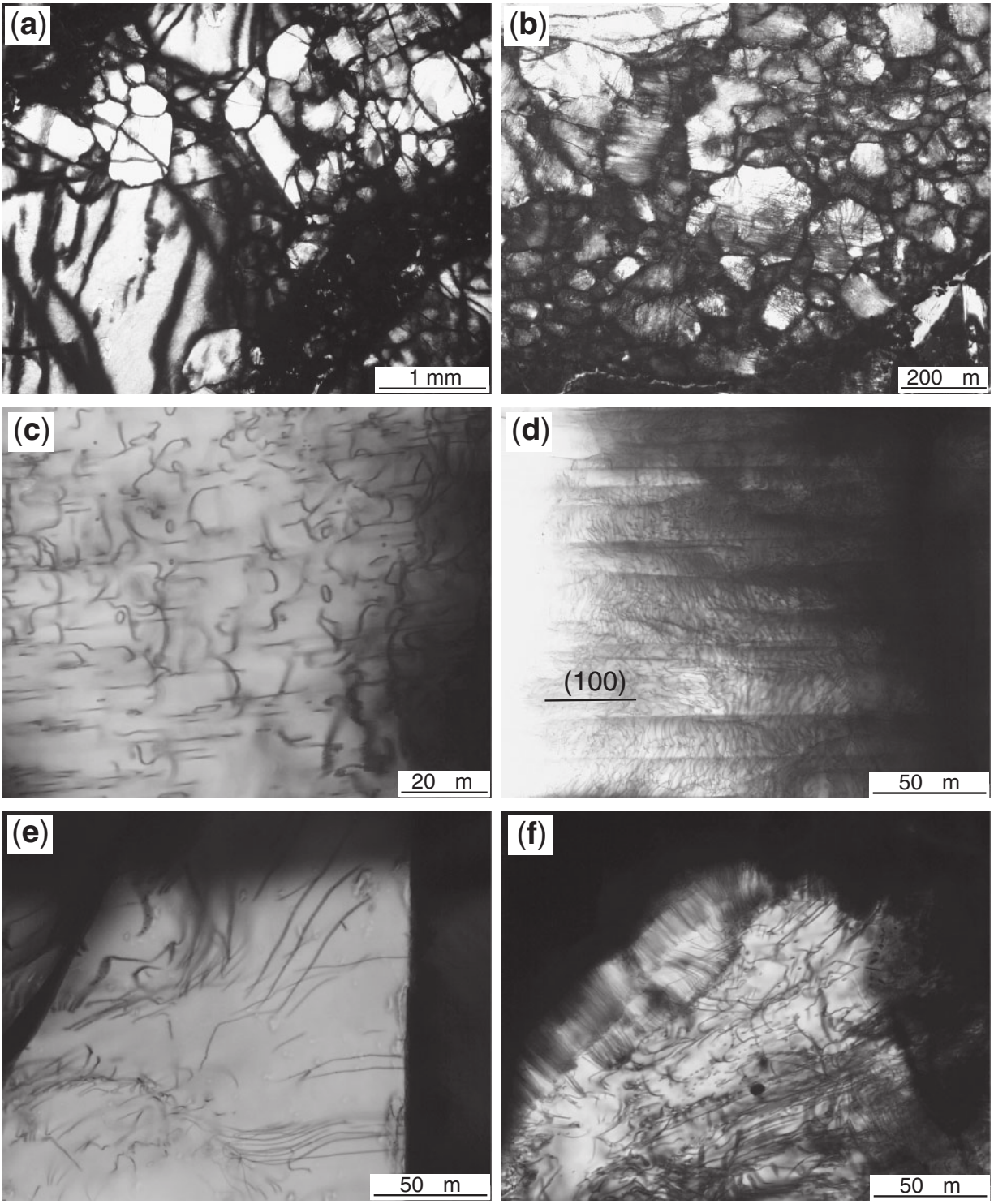

Fig. 6. Dislocation microstructures in NCR27 as observed on an oxidized thin section. (a) Multigranular olivine nodule. The discrepancy between the highly oxidized anhedral olivine and the tablets, and the higher oxidation along the microfractures, should be noted. (b) Recrystallized olivine grains in a nodule. Some are larger and display lower oxidation. (c) Dislocation loops within a deformed anhedral olivine. (d) Closely spaced (l00) dislocations walls in an anhedral olivine. (e) Tablet within an anhedral olivine. The large difference of dislocation densities as shown by the difference in oxidation, and the straight dislocation nearly perpendicular to the tablet margins, should be noted. (f) Matrix olivine showing a rim characterized by straight dislocations perpendicular to the olivine margins.

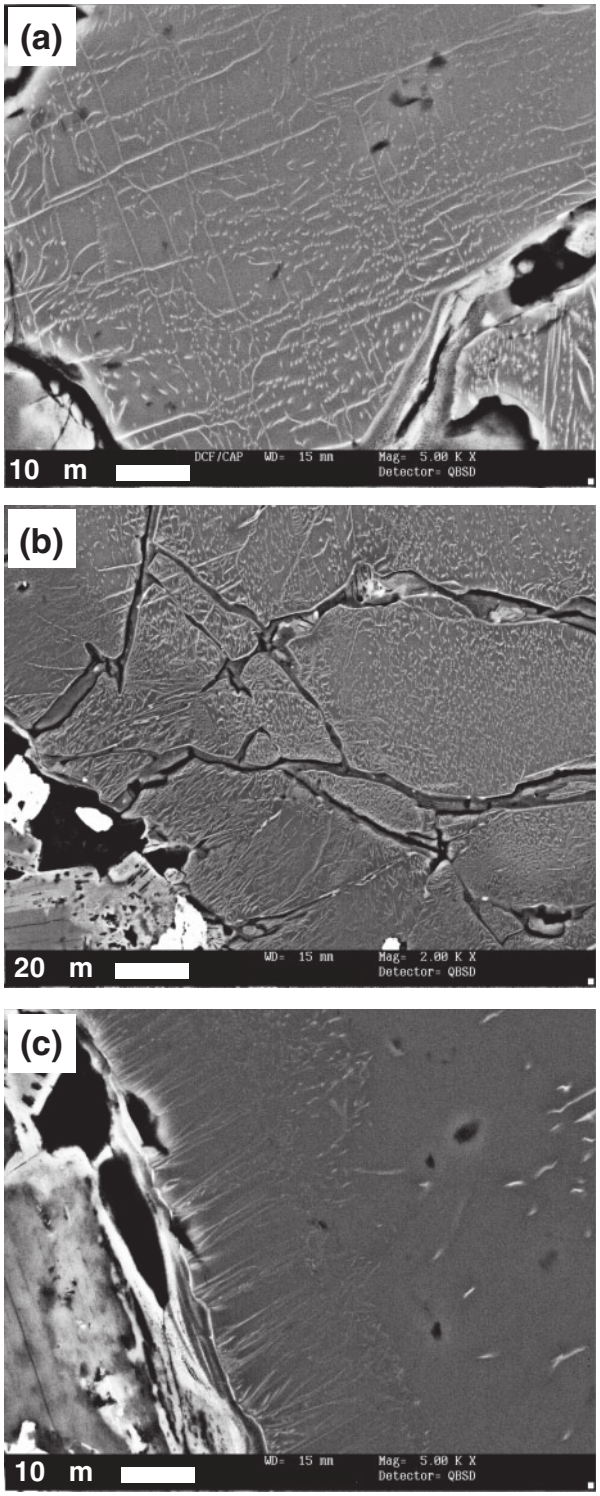

Fig. 7. Dislocation microstructures as observed on an oxidized thin section using an SEM in backscattered electron mode. (a) The central part of an anhedral olivine showing dislocations arranged within walls and free dislocations between these walls. (b) Matrix olivine with a lighter core displaying a high dislocation density surrounded by a darker rim displaying straight dislocations. (c) Rim of an olivine nodule showing straight dislocations.

We have also observed the oxidized thin sections with an SEM under backscattered mode following the method of Karato (1987), and the dislocations appear as white lines. The dislocations in anhedral olivine grains are clearly organized in walls, and free dislocations are present between these walls (Fig. 7a). The average density of free dislocations in anhedral olivine was measured at $2 \times 10^8\,\mathrm{cm}^{-2}$. The dislocation density is much lower in tablets (*c.* $10^7\,\mathrm{cm}^{-2}$ or lower) than in the anhedral olivine grains, thus confirming the observations made with a petrographic microscope. In addition, the cores of the matrix olivines also display a high density of dislocations (Fig. 7b). The rims of both the anhedral (Fig. 7b) and matrix olivine (Fig. 7c) show abundant straight dislocations nearly perpendicular to grain margins.

Because oxidation of the olivine crystals may be heterogeneous in the olivine grains (see Fig. 6a), and does not permit characterization of glide systems, TEM observations were performed on a normal thin section of a multigranular olivine nodule (Fig. 8a) to compare the dislocation microstructures in the anhedral olivines with those in the tablets. Numerous (001) and rare (100) dislocation walls were observed in the anhedral olivines. The density of free dislocations between these walls is $10^8\,\mathrm{cm}^{-2}$, much higher than in the tablets (less than $10^6\,\mathrm{cm}^{-2}$, Fig. 8b). Our observations and measurements on dislocation microstructures and density, spacing between dislocation walls and dynamically recrystallized grain size are consistent with those made by Guéguen (1977, 1979) and by Drury & Van Roermund (1989).

OLIVINE COMPOSITIONS

A distinctive and petrogenetically important characteristic of olivine in almost all the kimberlites in our collection is the wide range in Fo contents, as can be seen in Figs 9 and 10 and Supplementary Data Table S2. The greatest range was found in the Greenland sample NCR29, where Fo contents vary from 81·7 to 91·5 (Fig. 9 and Table 1) with no obvious correlation with morphology or grain size. A slightly smaller range is observed in NCR27 (from 85·3 to 91·7) but in this sample the distribution of compositions is more complicated. Fo contents are uniform within single nodules but vary widely from nodule to nodule. In the example shown in Fig. 10a and b, for example, the forsterite content of tablets and anhedral olivines within a single nodule varies only from 90·4 to 90·9, within the limit of error of the microprobe analyses. In contrast, from nodule to nodule, the Fo contents vary widely, as illustrated in Fig. 10a and in the X-ray microfluorescence maps reproduced in Fig. 11. The thin outer rims have contrasting and more complex variations, as discussed below.

Although we have not analysed other kimberlite samples in such detail, their olivines appear to share many of the

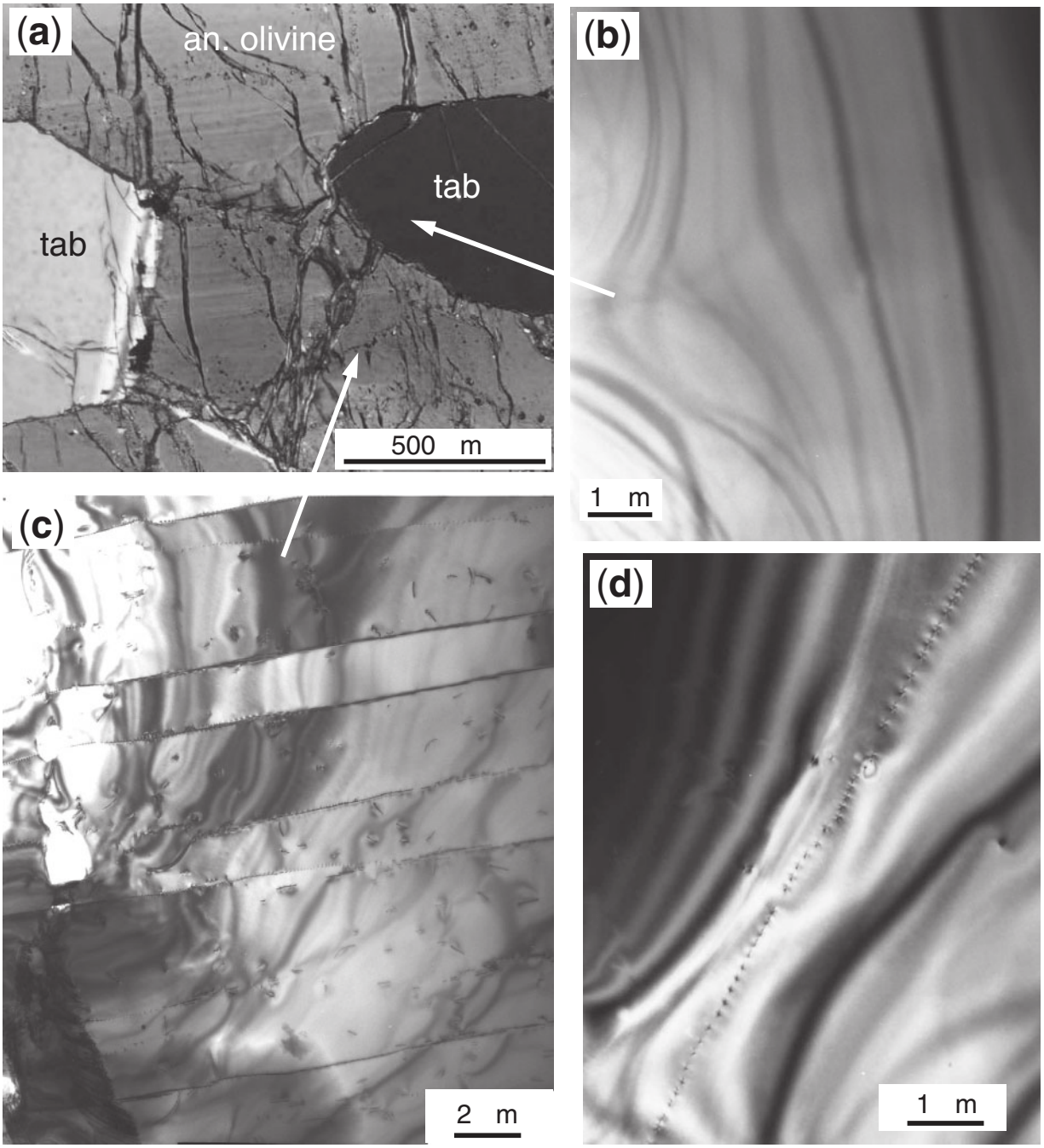

Fig. 8. Dislocation microstructures in an olivine nodule from NCR27 as observed with a TEM. (a) General view of the deformed anhedral olivine with two tablets. The closely spaced subhorizontal subgrain boundaries and the numerous small fluid inclusions in the anhedral olivine should be noted. (b) Tablet: no dislocation is visible in this image. (c) Anhedral olivine: closely spaced (l00) tilt dislocation walls and numerous free dislocations. (d) Detail of a (l00) dislocation wall.

geochemical characteristics of the Greenland samples. Olivine compositions are near constant within single nodules or multigranular aggregates in samples Plt-17-03 from Botswana and CRC-7a from the Finsch mine, but once again the compositions vary from nodule to nodule. The range is almost as large as in the Greenland samples; for example, from Fo82·4 to Fo92·7 in the sample with multigranular nodules, Plt-17-03 from Botswana (Fig. 9). In the Group II sample, CRC-7A from the Finsch Mine, the range is more restricted and compositions are more

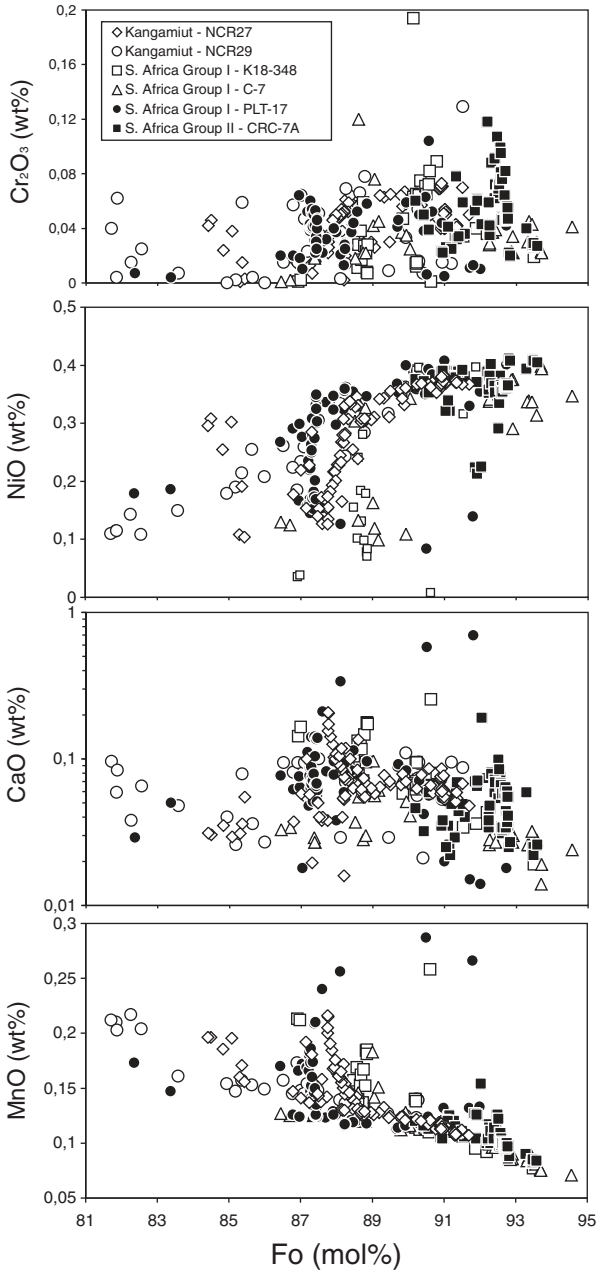

Fig. 9. Compositions of olivines in kimberlites. Fo vs Cr_2O_3, NiO, CaO and MnO.

magnesian, from Fo90·6 to Fo93·5. Similar ranges of compositions have been reported in kimberlites from other regions such as in the Diavik mine in Canada (Brett *et al.*, 2009) and the Udachnaya-East kimberlite (Kamenetsky *et al.*, 2008).

The chemical maps of Fe in four of our kimberlites (Fig. 11) illustrate another distinctive and important feature of the olivine compositions. In addition to demonstrating the wide range in Fo contents in all four samples, the maps show that surrounding many, but not all, of the olivine grains are narrow rims, from ~30 μm to more than 200 μm wide, whose composition differs from that of the olivine in the interior of the grain. The nature of the zoning is shown in more detail in the profiles reported in Fig. 12 and the sketch shown as Fig. 13. The four profiles were measured at the margins of four nodules in the Greenland kimberlite NCR27. In profile 1, the composition remains constant because the profile did not reach the outer margin of the grain. In profile 2, the olivine in the interior of the nodule has the composition Fo91, very similar to that of the first, but within the 110 μm wide rim, the Fo content declines, abruptly in a first step then more gradually in a second step, to a minimum value of Fo87·5. In this profile, the NiO content declines in an irregular manner, to reach a minimum value of 0·13% as the CaO and MnO contents both increase markedly. Cr_2O_3 first increases then decreases. In profile 3, the Fo, NiO and Cr_2O_3 contents initially increase, then decrease, whereas CaO and MnO increase progressively. It is notable that in the inner part of this profile, the Fo content is higher than that in the interior of the nodule. In profile 4, Fo contents first fall rapidly to very low values (near Fo84) then increase; the other elements vary in an irregular manner. These variations in Fo content and minor elements are very similar to those reported by other authors (e.g. Fedortchouk & Canil, 2004; Kamenetsky *et al.*, 2008; Brett *et al.*, 2009).

In the Fo vs NiO diagram (Fig. 9), most of the data plot on a broad array in which NiO correlates positively with Fo content. In most samples, the interiors of both nodules and matrix grains have Fo contents between 87 and 92; sample NCR29 extends the range to lower values and sample CRC-7a extends the range to values above Fo93. Falling off this trend are the compositions of the outer rims, whose NiO contents are relatively low. In the Group I kimberlites, the rims normally have compositions in a narrow range from about Fo87 to Fo89; in sample CRC-7a, the Group II kimberlite from the Finsch Mine in South Africa, the rims are more magnesian, with Fo contents between Fo92 and Fo93, corresponding to the generally higher Fo contents in the interiors of the olivine grains.

The other panels in Fig. 9 show that the CaO, MnO and in some cases Cr_2O_3 contents are relatively low in the interiors of nodules and somewhat higher in the rims. Compared with the compositions of olivine from the suite of mafic and ultramafic rocks analysed by Sobolev *et al.* (2007), the olivines in kimberlites have low contents of CaO, MnO and Cr_2O_3. Only their NiO contents are at levels similar to those of the magmatic olivines in the reference suite. Because of their low CaO and MnO contents, the compositions of kimberlitic olivines plot well outside the fields in the discrimination diagrams of Sobolev *et al.* (2007).

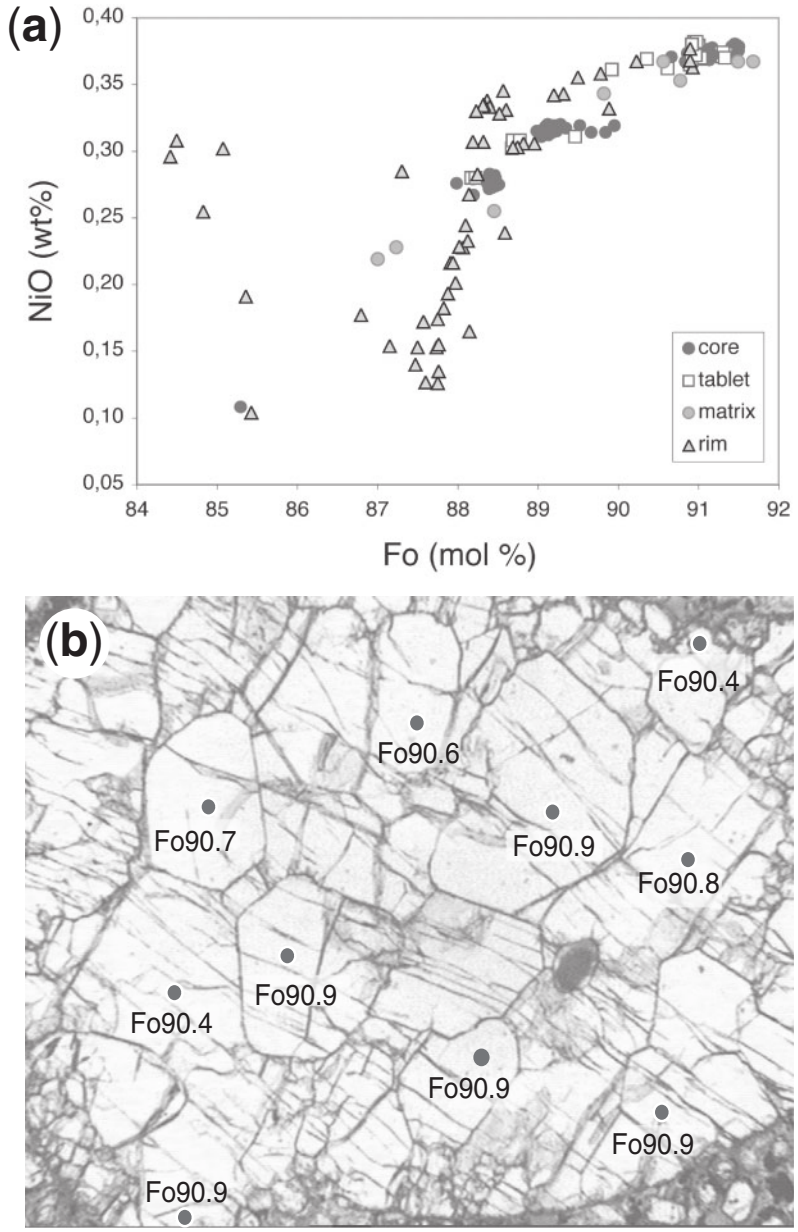

Fig. 10. Compositions of olivine in nodules of NCR27. (a) Fo vs NiO showing large variation in composition from nodule to nodule; (b) thin section photomicrograph of a nodule and compositions of tablets and anhedral grains.

DISCUSSION

Origin and evolution of the nodules

On the basis of our study of the kimberlites of our sample suite, combined with data from the literature, we conclude that olivine nodules are a feature of kimberlites worldwide. This leads us to believe that they are produced by a process that is linked directly to the formation of the kimberlite magmas themselves. To explain the nodules we have to account for the following observations.

(1) With very rare exceptions the nodules are monomineralic. Olivine is the sole mineral in the vast majority, and in those examples that contain another phase, that mineral appears to have been out of equilibrium with both the olivine and the kimberlite melt. The reaction rims around garnet and orthopyroxene macrocysts and the rounded orthopyroxene grain in Fig. 4e provide evidence of disequilibrium.

(2) Although many nodules consist of a single large crystal, others contain two or more grains, forming what

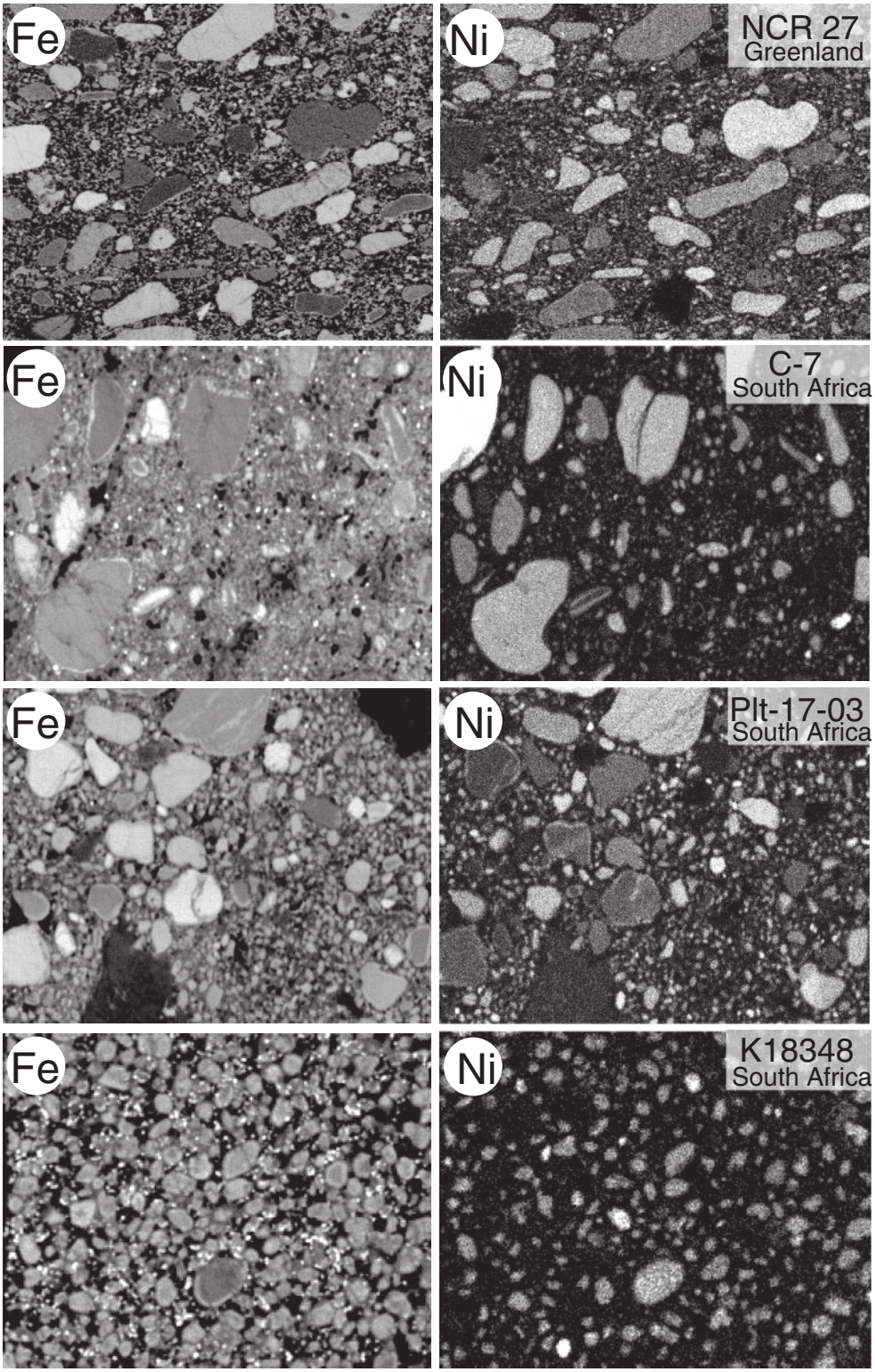

Fig. 11. Microfluorescence chemical maps showing the variations in Fe and Ni contents of olivine in four kimberlites. The wide variations in Fe and Ni contents and the inverse correlations between these two elements in all samples except for K18-348 should be noted. In K18-348 the core of the largest grain has a lower Fe content (high Fo) but the other grains have relatively constant compositions.

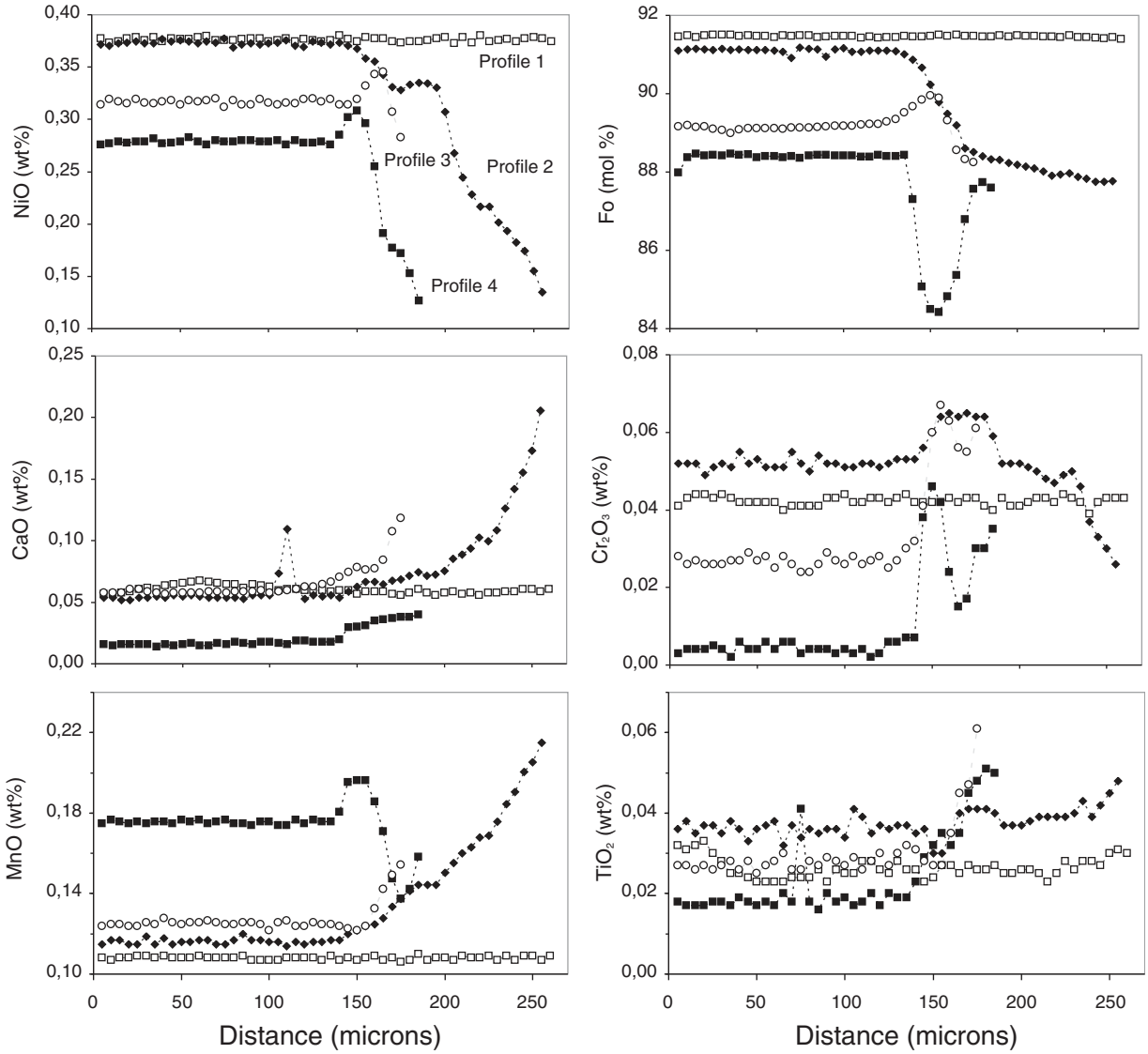

Fig. 12. Variations in the concentrations of major and minor elements and Fo contents in olivine at the margins of four nodules in sample NCR27.

we refer to as multigranular nodules. In sample NCR 27, such nodules constitute about 30% of the total population; in other samples the proportion ranges from 0 to about 20%. In the multigranular nodules, two types of olivine can be distinguished. The first comprises the small mosaic-textured grains in deformation corridors and the tablets, which, for reasons developed below, we believe to have formed by solid-state recrystallization. The second type is the anhedral olivine between the tablets. The observation that the deformation structures and the intergrain contacts are cut by the tablets indicates that the anhedral grains were present before the growth of the tablets. This tells us that the material that became the source of the nodules was itself multigranular; in other words, at least some of the multigranular nodules are xenoliths, not xenocrysts. Given their monomineralic nature and the presence only of olivine, the original rock type was dunite. In the case of monogranular nodules, the arguments for a xenolithic source are less obvious, but given that the size and range of compositions of the single crystals is similar to that of single grains in multigranular nodules and that olivine is by far the most abundant mineral in these kimberlites, it is most probable that the monogranular nodules were also derived from a source of essentially dunitic composition.

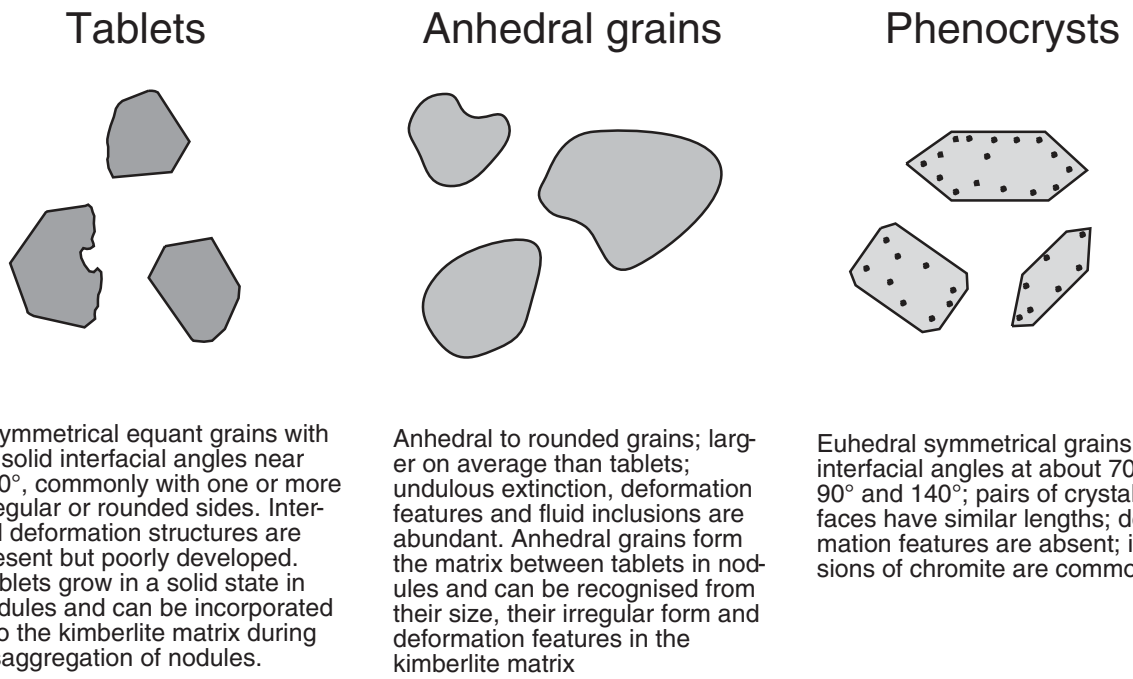

Fig. 13. Criteria that can be used to distinguish tablets, anhedral grains and phenocrysts.

(3) The composition of olivine in the majority of kimberlites in our sample suite varies widely. The uniform compositions within single nodules contrast with the wide range of variation from nodule to nodule, and within grains in the matrix. The near-identical composition of tablet, mosaic and anhedral olivine in single nodules supports the interpretation that the first two types of olivine formed by recrystallization of anhedral olivine. The large range of Fo contents (e.g. from Fo81·7 to 91·5 in NCR29 and from 85·3 to 91·7 in NCR 27) provides an important clue to the nature of the process that produced the dunitic source of the nodules, as discussed below.

(4) The concentrations of Ca, Mn and Cr in nodule and matrix olivine are extremely low. They are comparable with levels measured in olivine in xenoliths from the lithospheric mantle, but far lower than in magmatic olivines from mafic and ultramafic magmas (Kohler & Brey, 1990). In the thin rims surrounding some of the olivine nodules or grains in the matrix, CaO contents are higher; they approach, but do not reach, the levels in olivine in common basalts (Sobolev *et al.*, 2007).

(5) The deformation features in the olivine grains indicate that the dunite had been deformed before it was incorporated into the kimberlite. The deformation is similar in peridotite xenoliths in kimberlites from numerous locations (Boullier & Nicolas, 1975; Guéguen, 1977; Drury & Van Roermund, 1989).

Significance of deformation structures

From the observation of the microstructures, we infer that the anhedral olivines in the nodules were deformed by dislocation creep before their incorporation in the kimberlitic magma. The glide system, as determined from the crystallographic orientation of the dislocation walls and their rotation axes, is mainly [100](010) and secondarily [100](001); this corresponds to high-temperature deformation (Carter & Avé Lallemant, 1970; Raleigh & Kirby, 1970). Both the spacing between the dislocation walls and the size of recrystallized olivine can be used as piezometers. The stress values calculated from the Karato *et al.* (1980) piezometer using the mean subgrain size or the spacing between dislocation walls (5 μm) are in the 100–400 MPa range. Based on the mean size of dynamically recrystallized olivine grains (25 μm), and using the Karato *et al.* (1980) or Van der Wal *et al.* (1993) piezometers, the calculated stress values are in the 100–200 MPa range. We can then calculate the strain-rate using the flow law for dislocation creep in wet or dry dunite determined by Chopra & Paterson (1981, 1984) and considering a minimum temperature of 1200°C corresponding to the inflection point of the abnormal continental geotherm determined by Boyd & Nixon (1975) and MacGregor (1975). Depending on the flow law, the calculated strain-rate ranges from 5×10^{-5} to $3 \times 10^{-1}\,s^{-1}$ range in wet dunite and from 1×10^{-5} and $9 \times 10^{-9}\,s^{-1}$ in dry dunite. Strain-rates calculated using both piezometers and flow laws are far higher than those expected for convective

flow in the mantle (10^{-12} to 10^{-14} s^{-1}). The difference is increased if we consider a higher temperature of deformation (1400°C) corresponding to the most deformed peridotite xenoliths in kimberlites (Boyd & Nixon, 1975; MacGregor, 1975). This means that the high stress and high strain-rate deformation observed in the olivine nodules cannot have developed during steady-state convection-related flow in the mantle. Instead, and because the deformation of these nodules is similar to that in xenoliths from kimberlites all around the world (this work; Boullier & Nicolas, 1975; Guéguen, 1977, 1979) we believe that the deformation was a transient phenomenon that was directly linked to the formation of the kimberlite magmas themselves. Below, we attribute the deformation to the infiltration of proto-kimberlitic fluid into the base of the lithosphere.

The euhedral tablets in the olivine nodules cut across all the deformation microstructures (Figs 1b, 4d and 8a) and therefore postdate the deformation. Similar tablets have been described by various researchers in peridotite xenoliths from South African kimberlites (Boullier & Nicolas, 1975; Mercier & Nicolas, 1975; Green & Guéguen, 1983; Drury & Van Roermund, 1989) and have been experimentally reproduced by Nermond (1994) by static recrystallization, at 1200 or 1270°C and high confining pressure, of olivine crystals previously deformed under high stress and at low temperature. Following all these researchers, we interpret these tablets as having resulted from solid-state recrystallization during upward transport of the nodules within the kimberlitic magma. Drury & van Roermund (1989) suggested that the growth of tablets occurs by fluid-assisted grain boundary migration when a thin fluid film is present along the grain boundaries. The infiltration of fluid from the kimberlitic magma may have enhanced the disaggregation of the nodules and the incorporation of tablets and anhedral olivine grains into the kimberlitic magma.

Tablet growth is thought to occur during the first stages of kimberlite ascent because the tablet margins are cut by the rounded outer border of the nodules (Figs 1b and 4d). In such cases, the tablets first grew and then their margins were abraded as the nodules were transported upwards within the turbulently flowing kimberlite. The straight dislocations (Figs 6e, f and 7c) observed on the margins of both tablets and nodules are similar to growth dislocations formed in synthetic hydrothermally grown quartz crystals (Michot *et al.*, 1984). We suggest that these dislocations formed during solid-state growth of the tablets by migration of their fluid-rich grain boundaries, as previously proposed by Drury & van Roermund (1989). In the annealing experiments of Nermond (1994) tablets appeared in deformed olivine after 7 min of annealing. Thus, by comparison with these results, the growth of tablets in the anhedral olivine during their transport in the kimberlitic magma may also have been very rapid. High ascent rates of kimberlitic magma have also been inferred on the basis of hydrogen diffusion profiles in xenolithic mantle olivines from southern African kimberlites (5–37 m s^{-1}, Peslier *et al.*, 2008) and fluid mechanics calculations (30–50 m s^{-1}, Wilson & Head, 2007).

Similar structures are also present in matrix olivines. Straight dislocations normal to the margins, like those in the olivine nodules, are well developed on the margins of the matrix olivine grains, and the cores of these grains display dislocation microstructures similar to those of anhedral olivine in the nodules. A difference in composition between the central part and the rim of these matrix olivines accompanies the straight dislocations. This indicates that, as with the olivine nodules, most of the matrix olivine is also xenocrystic.

Interpretation of olivine grains in the matrix of kimberlites

According to Mitchell (1986, 1995) and many other kimberlite authorities, a euhedral form is one of the criteria that distinguish phenocrysts from xenocrysts. In our opinion, this criterion applies only in specific cases and cannot be used for the majority of kimberlites. In Fig. 13 we provide quantitative data on the size and form of olivine grains in the matrix of several kimberlites and compare them with tablets in the olivine nodules. In Fig. 14 we list the characteristics that can be used to distinguish between the three dominant types of olivine observed in kimberlites: tablets and anhedral olivine in nodules, and phenocrysts.

In Figs 1, 2, 4 and 14 we show that the olivine tablets have a distinctive morphology: they are near equant and commonly have crystal faces at an internal angle that varies from 120° to 140°; in most tablets the lengths of the crystal faces vary significantly to give the grains a non-symmetrical form; and commonly one or more faces of the tablet are irregular or rounded (Fig. 4a–d). The form of olivine phenocrysts in basaltic lava is different from those of the tablets. In their ideal form, as illustrated by the grain in a basaltic pillow rim (Fig. 4f), phenocrysts are slightly elongated with an aspect ratio of about 2:1; they are commonly symmetrical about one or more axes, reflecting the orthorhombic crystal system of olivine, and angles between crystal faces cluster about two main internal angles at 110° and 140°. Figure 4b shows that the form of the grains in the matrix of the kimberlite sample NCR29 resembles more closely those of tablets than those of the phenocrysts.

We documented the similarity in the morphology of tablets and matrix grains by measuring the size and interfacial angles of the various types of olivine. In Fig. 3a and b we compare the maximum dimension and perimeter of the grains and show that those of the tablets and matrix grains are similar. The frequency peak in both histograms

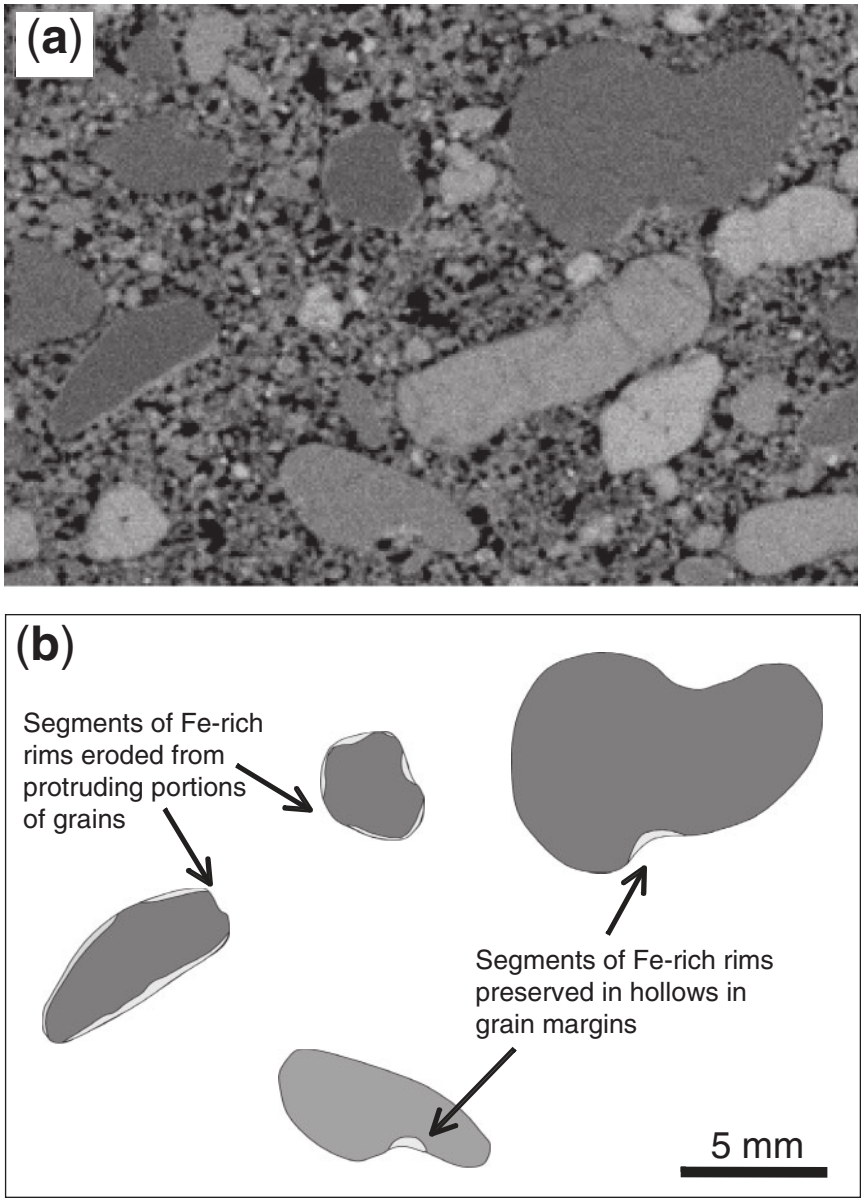

Fig. 14. (a) Microfluorescence map showing variation in the FeO content of nodules in sample NCR27; (b) sketch of several nodules showing the irregular distribution of Fe-rich rims.

is at a slightly higher value for both parameters, indicating that the average size of grains in the matrix is slightly greater than that of the tablets. A possible explanation for this difference could be that additional olivine has been added to grains in the matrix during growth of the outer olivine rims. This effect should, however, have been counterbalanced by the abrasion that rounded the outlines of many grains in the matrix. It is difficult to evaluate the relative magnitudes of the two opposing processes. Another, more likely, explanation is that some of the anhedral olivine from nodules, which normally has a larger grain size than the tablets, was included amongst the data representing matrix olivine grains compiled in Fig. 3a and b.

Measurements of interfacial angles are shown in Fig. 3c and d. Here we see that both the tablets and the grains in the matrix of samples NCR27 and NCR29 have a single prominent peak at about 140°, like that of the tablets, whereas the phenocryst in the pillow rim has peaks at 110° and 140°. The same morphology is found in sample K18-348, in which many grains are symmetric and have a form like those in picritic lavas. As in the picrites from La Réunion studied by Albarède *et al.* (1997), a large

proportion of the olivine in sample K18-348 is xenocrystic, as demonstrated by dislocation features in many of the cores of these crystals. However, the outer form of the crystals is probably controlled by the growth of new olivine around xenocrystic nuclei as in olivine grains in the Udachnaya-East kimberlite described by Kamenetsky *et al.* (2008) and in the Diavik kimberlite described by Brett *et al.* (2009).

Figures 10 and 12 show how the compositions of olivine relate to crystal form. In sample NCR27, the range of compositions of tablets is very similar to that of equant, asymmetrical olivine in the matrix: in both cases the Fo content varies widely and continuously, from Fo88·2 to 91·5 in tablets compared with Fo87·0 to 91·7 in matrix grains. The same range of variation is displayed in most other kimberlite samples, but not in K18-348 where the range of Fo contents is generally small, except for the conspicuously Fo-rich cores of some larger grains (Fig. 11)

On the basis of both the morphological and compositional data, we conclude that the majority of grains in the matrix of samples such as NCR27 and probably those in many other kimberlites, were derived from disaggregated nodules. The disaggregation probably took place during transport within the kimberlite magma, perhaps facilitated by infiltration of fluid from the kimberlite. Disaggregation is 'caught in the act' in the images shown in Figs 2f and 4a. In both images, the original outline of the nodule is clearly discernible, but many of the grains at the margin have become detached. Had transport continued, all the grains in these nodules would have become dispersed into the kimberlite magma.

This conclusion has important implications. Euhedral morphology is not a reliable criterion for the identification of phenocrystic olivine, because in many cases this form is acquired during growth of tablets within dunitic nodules; that is, by solid-state growth within xenoliths. In the majority of kimberlites, most of the olivine in the matrix is xenocrystic: many or most euhedral grains come from disaggregated nodules, and the rounded grain either are anhedral grains from nodules or they acquired this form during transport in the kimberlite magma.

Origin of the olivine rims and compositions of kimberlitic melts

The rims of olivine surrounding both nodules and matrix grains probably formed by crystallization of the kimberlitic liquid. As can be seen in Figs 9 and 11, they are present at the margins of some, but not all, grains in most samples. Continuous rims entirely surround some grains, whereas in others the rim is discontinuous and present only along segments of the grain margin. Figure 4d and the SEM images of Fig. 7 show that an outer rim has developed on the rounded outer margin of two multigranular nodules. The rim cuts indiscriminately across tablets and anhedral grain boundaries, indicating that the rims grew after the tablets had formed and after the nodule margin had been abraded. If we accept that the rounding of nodule margins resulted from mechanical abrasion during transport, this places the timing of rim growth after the start of transport of the nodule in turbulently flowing kimberlitic magma. In contrast, other nodules, such as the large peanut-shaped example in NCR27 (Figs 11 and 14), retain only a small rim segment that is restricted to concave portions of their margins. On other grains the rim is absent from the protruding segments of the margins, those parts that would be most susceptible to abrasion. We interpret this geometry to indicate that a pre-existing rim has been abraded away from exposed segments of the margins of many nodules, being retained only along protected segments. If this interpretation is correct, it means that part of the rims grew before the transport-related abrasion had terminated. Putting this together, we can conclude that the growth of olivine rims accompanied much of the upward migration of the kimberlite magma.

The compositions of the olivine rims are markedly different from that of olivine within the nodules. In many cases their Fo contents are lower than that in the nodules, as is illustrated by the bright rims in the Fe X-ray chemical maps (Fig. 11). However, in other cases, the rims are more magnesian than the cores. In sample NCR27, for example, most rims have Fo contents between 88 and 90 whereas the range in the nodules is from 85·3 to 91·7. In NCR29 the values are 85–89 in rims compared with 81·7–91·5 in the interior of the grains. In the Group II kimberlite CRC-7A, the rim compositions are notably more forsteritic, in the range 91–92, matching more closely that of the nodule olivine.

Figures 9 and 12 show that CaO and MnO contents in the rims in sample NCR27 are systematically higher than in the interiors of the olivine grains and NiO contents are lower. The CaO content of the rim olivine approaches that of magmatic olivine, in contrast to the very low CaO of olivine in xenoliths from the lithospheric mantle. The high CaO and MnO and low NiO, together with the position of the rims at the margins of the olivine grains and in contact with kimberlitic liquid, provides further evidence that the olivine in the rims is magmatic.

We can estimate the composition of the parental kimberlitic liquid from that of the rim olivine using the following procedure. We assume an Mg–Fe distribution coefficient of 0·5, as proposed by Dalton & Wood (1993) for CO_2-rich liquids, and we estimate the FeO content of the liquid on the basis of bulk-rock analyses of each sample. Although the presence of xenocrystic olivine causes the kimberlite to have a different bulk composition from that of the liquid, in our samples the FeO content of olivine and the bulk-rock are similar and we can use the FeO content of the bulk-rock to represent that of the liquid.

Table 2: Calculated MgO contents of kimberlitic liquids

	Kangamiut	Kangamiut	Group I	Group II
Fo*	89	90	89	92
FeO (wt %)†	11	11	8	7
MgO‡ (wt %); $K_D = 0{\cdot}5$	25·0	27·8	20·2	22·6
MgO‡ (wt %); $K_D = 0{\cdot}4$	20·0	22·2	16·2	18·0

*Average Fo content of olivine rims.
†FeO content estimated from bulk kimberlite composition.
‡MgO content estimated using Fo content and the given distribution coefficient.

The presence of abundant ilmenite macrocrysts would be problematic; however, most of our samples contain only a small amount of this phase. The <2% of ilmenite in sample NCR27 contributes less than 1% FeO to the bulk composition, which is within limits of the uncertainty of the FeO value. In addition, given the complexity of the zoning, as illustrated by the profiles in Fig. 12, the choice of olivine composition is not straightforward. We decided to choose a value corresponding to the inner part of the profile, but not the innermost points, which might sample material affected by diffusive transfer with xenocrystic olivine or by overlap of the microprobe beam. For the Greenland samples we calculated compositions using Fo contents of 89 and 90. As shown in Table 2 and Supplementary Data Table S2, this sample has a high FeO content of around 11 wt %, and because of this the estimated MgO content is also high, at 27·8 wt % for the olivine composition Fo90. If a lower forsterite content of Fo89 and a lower Mg–Fe distribution coefficient of 0·4 is chosen, the calculated MgO is 20 wt %. Sample NCR29 is near-aphanitic and its composition should be close to that of the liquid—the MgO content of the sample is 25·3 wt % MgO, in the middle of the range of the values that we calculated (Table 2 and Supplementary Data Table 2).

Typical Group I kimberlites from South Africa contain about 8 wt % FeO and if an olivine composition of Fo89 and an Mg–Fe distribution coefficient of 0·5 are adopted, the calculated liquid has a relatively low MgO of 20·2 wt %. The rims of olivine grains in Group II kimberlites are more magnesian, at about Fo92 (Fig. 9), but the bulk-rocks contain even lower amounts pf FeO of about 7 wt % (Mitchell, 1995). Our estimated liquid for the Group II kimberlites has an intermediate MgO of 22·6 wt %.

These MgO contents are slightly lower than those estimated by other workers. Price *et al.* (2000), le Roex *et al.* (2003) and Becker & le Roex (2006) obtained values of 21–30 wt % MgO for Group I kimberlites and 28–36 wt % MgO for Group II kimberlites on the basis of interpretation of trends in bulk-rock compositions. Kopylova *et al.* (2007) obtained 25·7–28·7 wt % MgO by analyzing the composition of the chilled margin of a Group I kimberlite dyke from the Jericho locality. The latter authors stated that the composition they estimated was 'too magnesian (Mg-number = 0·87) to be in equilibrium with the mantle'. This is true if an Mg–Fe distribution coefficient of 0·36 (from Herzberg & O'Hara, 2002) is assumed: use of this value yields Fo95 as the composition of the equilibrium olivine, whereas the olivine grains in their sample have the composition Fo91. If the procedure is reversed and the compositions of the dyke and the olivine are used to calculate the distribution coefficient, a value of 0·63 is obtained if all iron is assumed to be Fe^{2+}. If 10% of the iron is considered to be Fe^{3+}, the calculated distribution coefficient is 0·69. These values are at the upper limit of the coefficients proposed by Dalton & Wood (1993) for Mg–Fe partitioning between olivine and carbonate liquids. Either an unknown process enriched the kimberlite melt in Mg during its ascent from source to surface, as proposed by Kopylova *et al.* (2007), or the high coefficients are more appropriate for kimberlitic liquids.

In most samples the MgO content of the melt is far less than that of the bulk-rock, an observation that confirms the interpretation that most kimberlites contain a high proportion of xenocrystic olivine. We therefore concur with the conclusion of Brett *et al.* (2009) that the amount of phenocrystic olivine is commonly overestimated, but would take the argument further because, unlike them, we believe that most of the sub- to euhedral olivine is also xenocrystic, being derived from the matrix of dunitic xenoliths.

Source of dunite

The wide range from high to relatively low Fo contents (Fo82 to Fo93) indicates that the nature, and most probably the origin, of the dunitic rock that became the source of the nodules was very different from that of most other olivine-rich mantle rocks. In suites of peridotitic xenoliths from Precambrian subcontinental lithosphere, Fo contents

of olivine range from about Fo94 to Fo90, with very few values lower than Fo89 (Boyd, 1989). The same is true of olivine inclusions in diamonds, whose compositions fall in the range Fo96 to Fo90 (Stachel *et al.*, 2003). It is generally accepted that these Fo-rich olivines form as residues of very high degrees of mantle melting. Olivine in the xenoliths in picrites from East Greenland, for example, has a very uniform and highly forsterite-rich composition, close to Fo92·7, a composition that corresponds to a high degree of melting (about 40%) of normal mantle peridotite. Bernstein *et al.* (1998) pointed out that this degree of melting corresponds to the point at which orthopyroxene is eliminated, leaving only olivine in the residue. The most magnesian olivine in our kimberlite suites has a composition not far from this value, and this olivine could conceivably have formed through high-degree melting; however, the less magnesian olivines must have a different origin.

To explore this notion it is useful to estimate the composition of the liquids that might have crystallized the Fo-poor olivine. If, for example, we again adopt an Mg–Fe distribution coefficient of 0·5, as appropriate for the melting of mantle peridotite in the presence of CO_2 (Dalton & Wood, 1993), we can calculate a MgO/FeO of 0·8 for a melt in equilibrium with the olivine with the lowest Fo content (81·7). The aphanitic kimberlite NCR29 contains about 11% FeO, very similar to that of olivine with a composition Fo88, which is the average olivine composition in this sample. The high FeO contents of these rocks cause them to plot at the boundary between kimberlites and aillikites in the classification scheme of Francis & Patterson (2008). If the melt contained 11% FeO, then the melt in equilibrium with the Fo-poor olivine would have contained only about 8·8% MgO, which is far from the MgO content of high-degree mantle melts (Herzberg, 1995; Walter, 1999). Adopting the more usual Mg–Fe distribution coefficient of 0·3, as is appropriate for basaltic melts with low CO_2 contents, yields an even lower MgO content of about 5·5%. A melt containing 10% or less of MgO, if produced by partial melting of peridotite, would have had to form at shallow depths through low degrees of partial melting. Under these conditions several other mineral phases would also be retained in the residue of melting: in addition to olivine, there would be one or two pyroxenes and an aluminous phase. Melting under such conditions cannot produce the monomineralic dunitic lithology preserved in the kimberlitic nodules.

Another possibility is that the dunite formed as a cumulate during the crystallization of a mafic or ultramafic magma, perhaps in a lower crustal or upper mantle magma chamber. Here again the problem is the range of Fo contents. The more magnesian grains could conceivably have separated from a picritic to komatiitic liquid, but the less magnesian grains should have crystallized from a basaltic liquid. In normal circumstances pyroxene and other minerals would have crystallized together with the Fo-poor olivine. It is very difficult to imagine how olivine from cumulates derived from liquids of diverse compositions (low-Fo olivine from basaltic liquids, high-Fo olivine from picritic liquids) could have selectively been incorporated into a kimberlitic magma and how the co-crystallizing minerals could have been excluded.

On the basis of such arguments, and taking into account the fact that monomineralic, compositionally diverse nodules are found in kimberlites from many different regions, we conclude that the process that produced the dunite was different from normal mantle melting and crystallization. In the following section we argue that the dunite formed through a process that was directly linked to the interaction between proto-kimberlitic fluids and peridotite of the asthenospheric or lithospheric mantle.

Origin of kimberlite—constraints from the morphologies and compositions of olivine.

Kimberlitic magmas are thought to form through partial melting deep in the mantle (Eggler & Wendlandt, 1979; Wyllie, 1980; Canil & Scarfe, 1990; Dalton & Presnall, 1998). According to Kamenetsky *et al.* (2008), the initial melt or 'proto-kimberlite' is a chloride–carbonate-rich fluid with a very low SiO_2 content. During its passage towards the surface, its composition becomes more like that of kimberlitic magma as it interacts with its mantle wall-rocks: the assimilation of olivine and other mantle minerals increases the silica content of the fluid, driving it towards the low-SiO_2, high-MgO composition characteristic of kimberlite. Kamenetsky *et al.* (2004, 2008) used the compositions of pyroxene and garnet inclusions in olivine from the Udachnaya kimberlite to infer that the xenocrystic portions of these grains crystallized or equilibrated under conditions corresponding to the lower part of the lithospheric mantle, at 50 kbar and 900–1000°C. Our observations provide important constraints on how this olivine might have formed and important clues to the processes implicated in the formation and evolution of kimberlitic magmas.

The key observation is the xenolithic and dunitic nature of the nodules. The majority of kimberlite- or basalt-hosted xenoliths are lherzolites, harzburgites, pyroxenites or eclogites—rock types that contain significant amounts of ortho- and clinopyroxene and an aluminous phase such as spinel or garnet. In these rocks, olivine normally makes up less than 60% of the mineral assemblage. In contrast, olivine is the sole constituent of the vast majority of the nodules in the kimberlites. Orthopyroxene and garnet are present but rare, and, as mentioned above and shown in Fig. 4e, reaction zones or rounded margins indicate that these minerals were out of equilibrium with the kimberlite magma. Olivine, on the other hand, crystallized at the

borders of the nodules, indicating that it is a liquidus phase (along with phlogopite and perhaps ilmenite and chromite) during most of the evolution of the kimberlitic liquid.

It appears that an unknown process extracted minerals other than olivine from the material that was to form the nodules in the kimberlites. This process evidently acted before the passage of the kimberlite magma. It preceded the deformation that is recorded in the olivine grains, and certainly acted before the nodules were abraded to their rounded form. The process resulted in the crystallization of olivine (or recrystallization of pre-existing olivine) with a range of olivine compositions that is far greater—extending to lower Fo contents—than that normally recorded in peridotites from the lithosphere.

The compositions of kimberlites from different parts of the world define a series of trends that appear to be the result, at least in part, of the fractionation or accumulation of olivine (Mitchell, 1970, 1986; Arndt, 2003). The composition of the olivine that controls each trend corresponds to that of olivine in the lithospheric mantle through which the kimberlites passed on their way to the surface. The compositions of kimberlites that erupted on the Kaapvaal craton in South Africa are controlled by highly forsterite-rich olivine (Fo_{93}) plus highly Mg-rich orthopyroxene, with compositions similar to those occurring in mantle xenoliths from that region (Boyd & Mertzman, 1987; le Roex *et al.*, 2003). The compositions of kimberlites from post-Archean settings are controlled by less magnesian olivine, like that in xenoliths from younger cratons (Menzies, 1990), although those from off-craton regions in southern Africa also show evidence of orthopyroxene (plus phlogopite) accumulation in addition to olivine (Harris *et al.*, 2004). The lithospheric mantle beneath the Kaapvaal craton is unusually rich in orthopyroxene (Boyd & Mertzman, 1987; Griffin *et al.*, 1999), yet this mineral appears absent from the macrocryst assemblages and nodules in kimberlites. What appears to have happened is that the orthopyroxene has been resorbed, perhaps into the proto-kimberlite liquid, producing a hybrid magma in which olivine xenocrysts accumulated and from which olivine subsequently crystallized (Griffin *et al.*, 1999; le Roex *et al.*, 2003).

The notion that kimberlitic or proto-kimberlitic fluids react with mantle peridotite, eliminating pyroxene and leaving olivine, has been suggested in a number of recent publications. Brett *et al.* (2009) and Kamenetsky *et al.* (2008, 2009) have proposed that orthopyroxene dissolved into the kimberlite magma as xenoliths was transported to the surface. We also believe that mantle orthopyroxene reacted out, but we see this interaction happening earlier, before the xenoliths were entrained into the kimberlite magma. We emphasize again the monomineralic nature of the dunitic nodules and the variable Fo contents of their olivine, and argue that this association could not have been produced during entrainment of xenoliths in well-mixed, turbulently flowing magma.

We can only speculate on the exact nature of the process that initially produced the dunite. It probably was some type of metasomatism, perhaps resulting from the influx of CO_2–H_2O–Cl-rich fluids. However, rather than enriching the invaded rocks in incompatible elements and fluids—the role normally assigned to metasomatizing agents (Hawkesworth *et al.*, 1984; Grégoire *et al.*, 2003; Simon *et al.*, 2007)—these fluids extracted the more fusible or more soluble components from the rock, leaving behind olivine, the most refractory mineral. The process thus acted in the opposite sense to the normal conception of mantle metasomatism, in which relatively fusible minerals such as amphibole, clinopyroxene and garnet are added to refractory peridotite. The latter process is commonly called 'mantle fertilitization', reflecting the idea that the composition of the peridotite changes from refractory to one more capable of yielding basaltic partial melts. Adapting this idea, we introduce the term 'mantle defertilization' for the process that transforms lherzolite or harzburgite into refractory dunite. The process that best fits this behaviour is the type of interaction envisaged by Kelemen (1990) and Kelemen *et al.* (1998) between hydrous fluids and peridotite above subduction zones, or by Morgan & Liang (2003) for the interaction between basaltic melt and harzburgite beneath mid-oceanic ridges. In both situations, the peridotitic margins of the conduits through which the fluids pass become depleted in pyroxene and spinel and are thereby transformed into dunite.

A comparable process may have affected the rock that was later entrained as olivine nodules within the kimberlites. The SiO_2-poor chlorine–carbonate-rich proto-kimberlitic fluid was a potent metasomatic agent (Kamenetsky *et al.*, 2004), which reacted with and assimilated pyroxene and garnet from mantle peridotite, leaving behind olivine with diverse compositions (Kelemen, 1990; Shaw *et al.*, 1998). The interaction would have been facilitated by the unusual physical and chemical properties of these fluids: their low viscosity and their capacity to wet the surfaces of silicates allowed them to penetrate the wall-rocks, and the high reactivity of pyroxene and garnet with Si-undersaturated fluids facilitated the elimination of all minerals other than olivine (Drury & Van Roermund, 1989; Kamenetsky *et al.* 2004). The analyses by Morgan *et al.* (2008) of the margins of dunitic dykes in ophiolites and their experimental studies of melt–harzburgite interaction provide some clues about how these processes might have worked. A notable result is the wide variation in the Mg-number of olivine in the dunite: both in the natural example and in the experimental study, the dispersion of Mg-number was far greater in the dunite than in the original harzburgite. Morgan & Liang (2003) explained the variations in their experimental charges by modelling

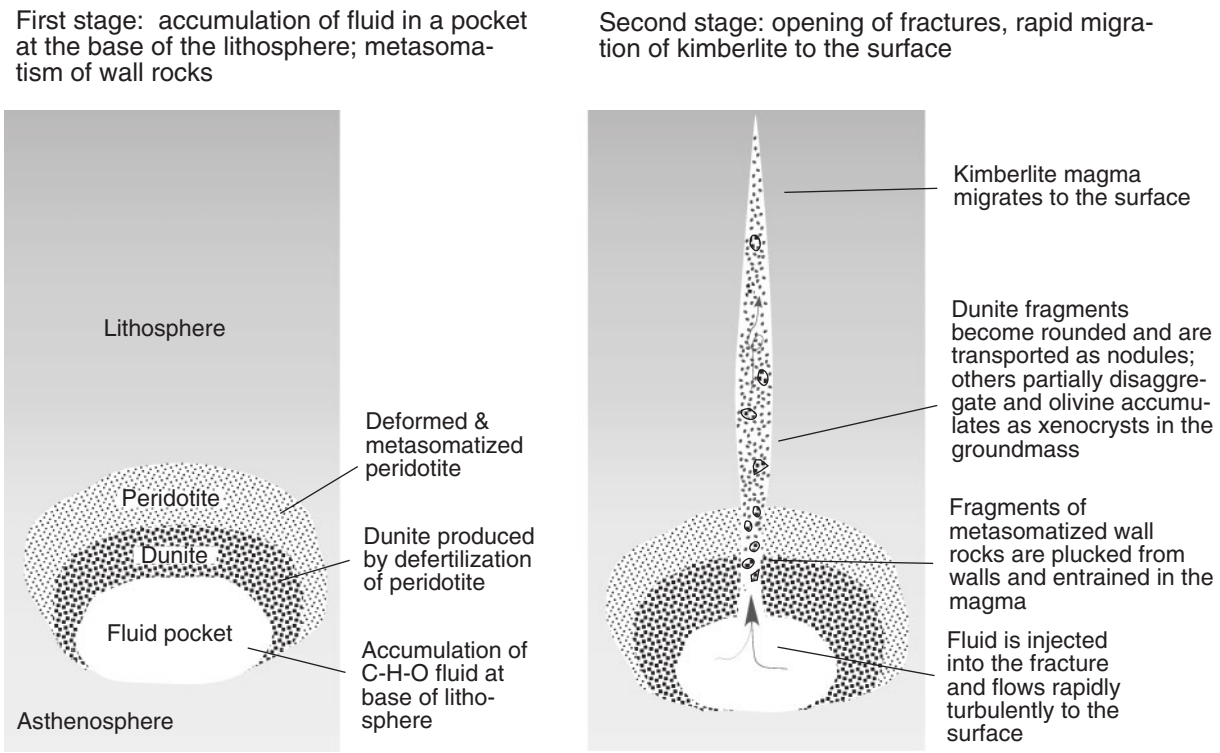

Fig. 15. Schematic illustration of the formation of kimberlites. In the first stage a CO_2-rich fluid generated deep in the mantle accumulates in a fluid-rich 'pocket' near the base of the lithosphere. The fluid interacts with surrounding rocks, reacting out pyroxene and garnet leaving only olivine. Deformation of the olivine in the dunitic reaction zone and surrounding peridotite occurs at this stage. In the second stage, build-up of pressure in the fluid pocket fractures the overlying peridotite. The fluid, now contaminated by the assimilation of pyroxene and garnet, enters the fracture and flows rapidly to the surface. It entrains fragments of the dunitic reaction sheath, which become rounded or disaggregate into isolated olivine grains. Higher up it also entrains and transports peridotite xenoliths.

diffusion of Mg and Fe between the reacting fluid and the ultramafic rock. Diffusion gradients are established in the reaction zones, and the form of these gradients depends on the relative levels of Mg and Fe in the fluid and wall-rock. As a result, Mg-number varies considerably over relatively short distances. In the dunitic bodies in the Josephine and Trinity ophiolites, variations in the Mg-number of olivine are irregular (Morgan & Liang, 2003), presumably because of variations in the lithology and physical properties (grain size, permeability) of the wall-rock. In each case the resultant dunite is monomineralic but displays a wide range in Fo contents, just as in the olivine nodules in kimberlites.

We envisage a proto-kimberlitic liquid that had a relatively low Mg-number, perhaps because it was derived from eclogite or another material with a relatively high FeO content (Gaffney *et al.*, 2007). Comparison can be made with C–H–O fluids in inclusions in diamonds and in olivine grains in kimberlites, in which Mg-number ranges widely from about 59 to 82 (Klein-BenDavid *et al.*, 2004). We speculate that the proto-kimberlitic fluid reacted with its mantle wall-rocks to produce a sheath of metasomatized, defertilized material whose composition ranged from dunite adjacent to conduit boundaries to lherzolite farther from the contact (Fig. 15). The composition of olivine within the reaction zone varied from Fe-rich values appropriate for olivine in equilibrium with the fluid adjacent to conduit boundaries, to values close to those of the original mantle rock farther away. The dunite material that formed through reaction with the proto-kimberlite liquid was subsequently incorporated into the kimberlite magma and transported to the surface. Stresses imposed by the influx of the proto-kimberlitic fluid caused some of the deformation recorded in olivines now in the kimberlites.

What is implied is a sequence of events that starts with interaction between fluid and rock—a relatively protracted process during which the major and trace elements had time to diffuse into and from the wall-rocks. This was followed by a more dynamic event during which the wall-rock was disrupted and entrained into the kimberlite magma. The fact that dunitic nodules are found in kimberlites worldwide indicates that the association of the two events is not coincidental, and is most probably an integral part of the generation of kimberlites.

Green & Guéguen (1974) and Grégoire *et al.* (2006) described situations in which these events might have taken place. Green & Guéguen (1974) proposed that a density instability forms deep in the mantle and becomes a diapir driven by the buoyancy force. At a shallower level it reaches the solidus and partially melts to form kimberlitic magma. Grégoire *et al.* (2006) envisaged the generation of proto-kimberlitic fluids deep within the mantle, perhaps within the Transition Zone, and upward migration of these fluids aided by compaction of the peridotite matrix. On reaching the base of the lithosphere the fluids segregate into kilometre-scale 'mush–melt' pockets. The fluids accumulate in these pockets until the build-up of internal pressure opens fractures in the overlying, rigid lithospheric mantle. With release of pressure the kimberlitic magma migrates rapidly through the fractures to the surface.

We associate an initial period of fluid–rock interaction with the accumulation of fluid in the 'mush–melt' pockets. We are unable to define the geometry of these melt pockets or the dynamics of the process, but propose that at this stage mantle peridotite was 'defertilized' and deformed. During the upward ascent of the fluid through fractures that opened in the upper carapace, the kimberlite magma plucked off fragments of wall-rock, initially the dunite from the inner lining of the metasomatic zone around the melt pocket, subsequently metasomatized peridotite from the outer carapace and finally unmetasomatized peridotite from higher in the lithosphere. The flow in the kimberlite was rapid (5–37 m/s, Peslier *et al.*, 2008; 30–50 m/s, Wilson & Head, 2007) and turbulent, and the fragments disaggregated and became rounded.

The tablets subsequently formed very rapidly as the grains were maintained at a high temperature in the kimberlitic magma. Olivine rims surround many but not all grains—both nodules and grains in the matrix. In most cases the rim was added to rounded outlines of the grain, indicating that the rim olivine grew after abrasion during transport. On the other hand, rims are absent from the outer margins of many other grains (Fig. 13), which indicates either that olivine did not grow there for some unknown reason, or that the rim was removed by abrasion. The highly irregular variations in the contents of major and minor elements in the rims are illustrated in Figs 9 and 12. These variations are taken as evidence that conditions fluctuated during growth of the olivine rims, perhaps as a result of changes in external parameters, particularly fluid pressure, or because of local heterogeneities in the composition of the liquid between the olivine grains.

GROUP I AND GROUP II KIMBERLITES

The accumulation of the pre-kimberlitic fluid that created the dunite, and the entrainment of the dunite nodules, took place within or below the lithosphere. Interaction between fluid and peridotitic wall-rock probably controls the trace element contents of kimberlites, as proposed by Khazan & Fialko (2005). When this interaction takes place entirely at sub-lithosphere depths, the kimberlite acquires an asthenospheric isotopic signature; when it occurs within the lithosphere, the isotopic signature will reflect this interaction. The CO_2 content of the parental magma might control the depth interval over which such interaction takes place and might therefore influence the isotopic compositions of kimberlites

In Group I kimberlites, which have asthenospheric Nd and Sr isotopic signatures and high CO_2 contents (see Becker & le Roex, 2006), exsolution might start at depths near the base of the lithosphere. Once a separate gas phase forms the magma will be driven rapidly to the surface, precluding subsequent interaction with the wall-rocks. These magmas retain the isotopic signature of the asthenosphere. The relatively low MgO content of these kimberlitic liquids, as calculated from the compositions of the olivine rims, may be related to the modest Fo content of olivine in asthenospheric peridotite.

In Group II kimberlites, which generally have lower CO_2 contents, exsolution takes place at shallower depths, and the magmas interact with shallower mantle and acquire the lithospheric isotopic signature that characterizes this type of kimberlite. The high MgO content of the parental liquids of these kimberlites, again calculated from the compositions of the olivine rims, may be related to the higher Fo content of olivine in cratonic lithospheric mantle.

KIMBERLITES, NODULES, AND DIAMONDS

Diamonds are thought to form as a result of interaction between reduced methane–water-rich fluids and peridotite of the lithospheric mantle (Malkovets *et al.*, 2007). In some ways the process is comparable with the interaction of fluid and peridotite that produced the dunite that forms the nodules in kimberlites and it is tempting to associate the two; however, consideration of other data rules this out. Dating of inclusions in diamonds has shown that, with rare exceptions, the diamonds formed well before the intrusion of the host kimberlitic magmas. Shirey *et al.* (2002), for example, used the Re–Os method to establish that diamonds in southern Africa formed in a series of Archean and Proterozoic events that occurred well before the Devonian eruption of most of the kimberlites in that region. In addition, the metasomatism associated with the influx of fluids has contrasting effects on the peridotite: the diamond-forming reaction was part of a normal metasomatic process that transformed refractory harzburgite into more 'fertile' garnet-bearing peridotite, whereas the

reaction that precedes the generation of kimberlites removes garnet and pyroxene.

A possible link between the two processes might be found, however, if we consider what happens to the metasomatized rocks following their entrainment into the kimberlitic magma. Diamonds are xenocrysts that are recovered as isolated crystals in the kimberlite matrix: presumably they are derived from xenoliths of metasomatized peridotitic (or in some cases eclogitic) wall-rocks that disaggregated during transport to the surface. Our identification of euhedral olivine grains from disaggregated dunitic xenoliths in the matrix of kimberlite, and our observation of partially disaggregated nodules, tells us that a comparable process affected the dunitic xenoliths. The high abundance of xenocrystic olivine in kimberlites attests to the efficiency of the process. We speculate that the distribution and the abundance of diamonds in kimberlites (in other words, the ore grade of diamond deposits) may have been influenced by the same processes that ripped off fragments of dunite from the conduit walls, then disaggregated and redistributed them during the ascent of magma to the surface.

CONCLUSIONS

(1) The morphology and the range of chemical compositions of olivine in kimberlites is distinctly different from that of olivine in most other mantle rocks. Most of the kimberlitic olivine is xenocrystic and was derived from a dunitic source.

(2) The crystal faces of many sub- to euhedral olivine grains in the matrix of kimberlites developed during solid-state recrystallization of dunite before or during the passage of kimberlite magmas through the lithosphere. A euhedral habit is not necessarily diagnostic of a phenocrystic origin of olivine in kimberlites.

(3) The wide range of Fo contents of olivine in kimberlites indicates that the dunite formed neither as the residue of high-degree melting nor as a product of crystallization from the kimberlitic magma. The dunite was probably produced by a metasomatic 'defertilization' reaction during which a proto-kimberlitic C–H–O liquid reacted with mantle peridotite, extracting pyroxene and garnet and leaving olivine of diverse composition. This dunite was entrained into the kimberlitic magma where some of it survived as discrete nodules and other parts disaggregated to yield isolated olivine grains.

(4) The compositions of thin olivine rims that surround some olivine xenocrysts can be used to estimate the compositions of kimberlitic magmas. The MgO contents of these magmas range from about 15 to 25 wt %, far lower than the bulk-rock compositions, which are influenced by the presence of abundant xenocrystic olivine.

ACKNOWLEDGEMENTS

We thank many people who contributed to this study. Don Schissel provided the samples from Kangmiut, Ekati and Snap Lake, and Don Francis provided those from Somerset Island. Technicians and colleagues in universities throughout France and in Germany helped with numerous aspects of the preparation and analysis of samples: Francin Keller (trace elements, Grenoble); Mathieu Corazzi (microprobe, Grenoble), Francis Coeur (rock crushing, Grenoble), Daniel Arnaud (thin sections, Grenoble); Olivier Romeyer (SEM, Chambéry), Christophe Nevado (thin sections, Montpellier), Dmitry Kuzmin (microprobe, Mainz). Miguel Montes, Jean-Pierre Clément, Michel Dubois worked on specific aspects of the project. We also thank the journal reviewers, Dima Kamanetsky, Kelly Russell and Michel Grégoire, and acknowledge valuable discussions with Benoît Ildefonse, Leonid Danyshevsky, José Gaspar, Jean-Claude Mercier and Don Francis.

FUNDING

The work was supported by the Centre National de Recherche Scientifique (CNRS), Institut National des Sciences de l'Univers (INSU), which contributed research funds 75 and technical support. The TEM national facility in Lille is supported by the CNRS (INSU) and the Conseil Régional du Nord–Pas de Calais, France.

SUPPLEMENTARY DATA

Supplementary data for this paper are available at *Journal of Petrology* online.

REFERENCES

Albarède, F., Luais, B., Fitton, G., Semet, M., Kaminski, E., Upton, B. G., Bachèlery, P. & Cheminée, J.-L. (1997). The geochemical regimes of Piton de la Fournaise volcano (Rèunion) during the last 530 000 years. *Journal of Petrology* **38**, 171–201.

Arndt, N. T. (2003). Komatiites, kimberlites and boninites. *Journal of Geophysical Research* **108**(B6), 2293, doi:10.1029/2002JB002157.

Arndt, N. T., Boullier, A. M., Clement, J. P., Dubois, M. & Schissel, D. (2006). What olivine, the neglected mineral, tells us about kimberlite petrogenesis. *eEarth* **1**, 15–21.

Becker, M. & le Roex, A. P. (2006). Geochemistry of South African on- and off-craton, group I and group II kimberlites: petrogenesis and source region evolution. *Journal of Petrology* **47**, 673–703.

Bernstein, S., Kelemen, P. B. & Brooks, C. K. (1998). Depleted spinel harzburgite xenoliths in Tertiary dykes from East Greenland: restites from high degree melting. *Earth and Planetary Science Letters* **154**, 221–235.

Boullier, A. M. & Nicolas, A. (1975). Classification of textures and fabrics of peridotite xenoliths from south African kimberlites. *Physics and Chemistry of the Earth* **9**, 467–475.

Boyd, F. R. (1989). Compositional distinction between oceanic and cratonic lithosphere. *Earth and Planetary Science Letters* **96**, 15–26.

Boyd, F. R. & Mertzman, S. A. (1987). Composition and structure of the Kaapvaal lithosphere, southern Africa. In: Mysen, B. O. (ed.) *Magmatic Processes: Physicochemical Principles. Geochemical Society Special Publications* **1**, 13–24.

Boyd, F. R. & Nixon, P. H. (1975). Origins of the ultramafic nodules from some kimberlites of northern Lesotho and the Monastery Mine, South Africa. *Physics and Chemistry of the Earth* **9**, 431–454.

Brett, R. C., Russell, J. K. & Moss, S. (2009). Origin of olivine in kimberlite: Phenocryst or Imposter? *Lithos* doi:10.1016/j.lithos.2009.04.030.

Canil, D. & Scarfe, C. M. (1990). Phase relations in peridotite + CO_2 systems to 12 GPa: implications for the origin of kimberlite and carbonate stability in the Earth's upper mantle. *Journal of Geophysical Research* **95**, 15805–15816.

Carter, N. L. & Avé Lallemant, H. G. (1970). High temperature flow of dunite and peridotite. *Geological Society of America Bulletin* **81**, 2181–2202.

Chopra, P. N. & Paterson, M. S. (1981). The experimental deformation of dunite. *Tectonophysics* **78**, 453–473.

Chopra, P. N. & Paterson, M. S. (1984). The role of water in the deformation of dunite. *Journal of Geophysical Research* **89**, 7861–7876.

Dalton, J. A. & Presnall, D. C. (1998). The continuum of primary carbonatitic–kimberlitic melt compositions in equilibrium with lherzolite: data from the system CaO–MgO–Al_2O_3–SiO_2–CO_2 at 6 GPa. *Journal of Petrology* **39**, 1953–1964.

Dalton, J. A. & Wood, B. J. (1993). The partitioning of Fe and Mg between olivine and carbonate and the stability of carbonate under mantle conditions. *Contributions to Mineralogy and Petrology* **114**, 501–509.

Drury, M. R. & Van Roermund, H. L. M. (1989). Fluid assisted recrystallization in upper mantle peridotite xenoliths from kimberlites. *Journal of Petrology* **30**, 133–152.

Eggler, D. H. & Wendlandt, R. F. (1979). Experimental studies on the relationship between kimberlite magmas and partial melting of peridotite. In: Boyd, F. R. & Meyer, H. O. A. (eds) *Kimberlites, Diatremes, and Diamonds: Their Geology, Petrology, and Geochemistry*. Washington, DC: American Geophysical Union.

Fedortchouk, Y. & Canil, D. (2004). Intensive variables in kimberlite magmas, Lac de Gras, Canada and implications for diamond survival. *Journal of Petrology* **45**, 1725–1745.

Francis, D. & Patterson, M. (2008). Kimberlites and aillikites as probes of the continental lithospheric mantle. *Lithos* **109**, 72–80.

Gaffney, A. M., Blichert-Toft, J., Nelson, B. K., Bizzarro, M., Rosing, M. & Albarède, F. (2007). Constraints on source-forming processes of West Greenland kimberlites inferred from Hf–Nd isotope systematics. *Geochimica et Cosmochimica Acta* **71**, 2820–2836.

Green, H. W., II, Guéguen, & Y., (1974). Origin of kimberlite pipes by diapir upwelling in the upper mantle. *Nature* **249**, 617–620.

Green, H. W., II, Guéguen, & Y., (1983). Deformation of peridotite in the mantle and extraction by kimberlite: a case history documented by fluid and solid precipitates in olivine. *Tectonophysics* **92**, 71–92.

Grégoire, M., Bell, D. R. & Le Roex, A. P. (2003). Garnet lherzolites from the Kaapvaal Craton (South Africa): trace element evidence for a metasomatic history. *Journal of Petrology* **44**, 629–657.

Grégoire, M., Rabinowicz, M. & Janse, A. J. A. (2006). Mantle mush compaction: a key to understand the mechanisms of concentration of kimberlite melts and the initiation of swarms of kimberlite dykes. *Journal of Petrology* **47**, 631–646.

Griffin, W. L., O'Reilly, S. Y. & Ryan, C. G. (1999). The composition and origin of sub-continental lithospheric mantle. In: Fei, Y., Bertka, C. M. & Mysen, B. O. (eds) *Mantle Petrology: Field Observations and High-pressure Experimentation*. Houston, TX: Geochemical Society, pp. 13–46.

Guéguen, Y. (1977). Dislocations In mantle peridotite nodules. *Tectonophysics* **39**, 231–254.

Guéguen, Y. (1979). Dislocations in naturally deformed terrestrial olivine: classification, interpretation, applications. *Bulletin de Minéralogie* **102**, 178–183.

Hawkesworth, C. J., Rogers, N. W., Van Calsteren, P. W. C. & Menzies, M. A. (1984). Mantle enrichment processes. *Nature* **311**, 331–336.

Herzberg, C. (1995). Generation of plume magmas through time: an experimental perspective. *Chemical Geology* **126**, 1–17.

Herzberg, C. & O'Hara, M. J. (2002). Plume-associated ultramafic magmas of Phanerozoic age. *Journal of Petrology* **43**, 1857–1883.

Hutchison, M. T. (2008). Diamondiferous kimberlite from Garnet Lake, West Greenland I: genesis, geochemistry and emplacement. In: *9th International Kimberlite Conference Extended Abstracts*, No. 9IKC-A-00183.

Kamenetsky, M. B., Sobolev, A. V., Kamenetsky, V. S., Maas, R., Thomas, R. & Sobolev, N. V. (2004). Kimberlite melts rich in alkali chlorides and carbonates: A potent metasomatic agent in the mantle. *Geology* **32**, 845–848.

Kamenetsky, V. S., Kamenetsky, M. B., Sobolev, A. V., Golovin, A. V., Demouchy, S., Faure, K., Sharygin, V. V. & Kuzmin, D. V. (2008). Olivine in the Udachnaya-East Kimberlite (Yakutia, Russia): types, compositions and origins. *Journal of Petrology* **49**, 823–839.

Kamenetsky, V. S., Kamenetsky, M. B., Sobolev, A. V., Golovin, A. V., Sharygin, V. V., Pokhilenko, N. P. & Sobolev, N. V. (2009). Can pyroxenes be liquidus minerals in the kimberlite magma? *Lithos* 10.1016/j.lithos.2009.03.040.

Karato, S. (1987). Scanning electron microscope observation of dislocations in olivine. *Physics and Chemistry of Minerals* **14**, 245–248.

Karato, S. I., Toriumi, M. & Fujii, T. (1980). Dynamic recrystallizarion of olivine single crystals during high-temperature creep. *Geophysical Research Letters* **7**, 649–652.

Kelemen, P. B. (1990). Reaction between ultramafic rock and fractionating basaltic magma I. Phase relations, the origin of calc-alkaline magma series, and the formation of discordant dunite. *Journal of Petrology* **31**, 51–98.

Kelemen, P. B., Hart, S. R. & Berstein, S. (1998). Silica enrichment in the continental upper mantle via melt/rock reaction. *Earth and Planetary Science Letters* **164**, 387–406.

Khazan, Y. & Fialko, Y. (2005). Why do kimberlites from different provinces have similar trace element patterns? *Geochemistry, Geophysics, Geosystems* **6**, Q100, doi:10010.11029/12005GC000919.

Klein-BenDavid, O., Izraeli, E. S., Hauri, E. & Navon, O. (2004). Mantle fluid evolution—a tale of one diamond. *Lithos* **77**, 243–253.

Kohler, T. & Brey, G. P. (1990). Ca-exchange between olivine and clinopyroxene as a geothermobarometer calibrated from 2 to 60 kbar in primitive natural lherzolites. *Geochemica et Cosmochimica Acta* **54**, 2375–2388.

Kohlstedt, L. D., Goetze, C., Durham, W. B. & Vander Sande, J. (1976). New technique for decorating dislocations in olivine. *Science* **191**, 1045–1046.

Kopylova, M. G., Matveev, S. & Raudsepp, M. (2007). Searching for parental kimberlite melt. *Geochimica et Cosmochimica Acta* **71**, 3616–3629.

le Roex, A. P., Bell, D. R. & Davis, P. (2003). Petrogenesis of Group I kimberlites from Kimberley, South Africa: evidence from bulk rock geochemistry. *Journal of Petrology* **44**, 2261–2286.

MacGregor, I. D. (1975). Petrologic and thermal structure of the upper mantle beneath South Africa in the Cretaceous. *Physics and Chemistry of the Earth* **9**, 455–466.

Malkovets, V. G., Griffin, W. L., O'Reilly, S. Y. & Wood, B. J. (2007). Diamond, subcalcic garnet, and mantle metasomatism: Kimberlite sampling patterns define the link. *Geology* **35**, 339–342.

Marini, J.-C., Chauvel, C. & Maury, R. C. (2005). Hf isotope compositions of northern Luzon arc lavas suggest involvement of pelagic sediments in their source. *Contributions to Mineralogy and Petrology* **149**, 216–232.

Menzies, M. A. (1990). Archaean, Proterozoic and Phanerozoic lithospheres. In: Menzies, M. A. (ed.) *Continental Mantle*. Oxford: Clarendon, pp. 67–86.

Mercier, J. C. & Nicolas, A. (1975). Textures and fabrics of upper mantle peridotites as illustrated by xenoliths from basalts. *Journal of Petrology* **16**, 454–487.

Michot, G., Weil, B. & George, A. (1984). In situ observation by synchrotron X-ray topography of the evolution with temperature of fluid inclusions in synthetic quartz. *Journal of Crystal Growth* **69**, 627–30.

Mitchell, R. H. (1970). Kimberlites and related rocks—a critical appraisal. *Journal of Geology* **78**, 686–704.

Mitchell, R. H. (1978). Mineralogy of the Elwin Bay kimberlite, Somerset Island, N.W.T., Canada. *American Mineralogist* **63**, 47–57.

Mitchell, R. H. (1986). *Kimberlites: Mineralogy, Geochemistry, and Petrology*. New York: Plenum.

Mitchell, R. H. (1995). *Kimberlites, Orangites, and Related Rocks*. New York: Plenum.

Moore, A. E. (1988). Olivine: a monitor of magma evolutionary paths in kimberlites and olivine melilitites. *Contributions to Mineralogy and Petrology* **99**, 238–248.

Morgan, Z. T. & Liang, Y. (2003). An experimental and numerical study of the kinetics of harzburgite reactive dissolution with applications to dunite dike formation. *Earth and Planetary Science Letters* **214**, 59–74.

Morgan, Z. T., Liang, Y. & Kelemen, P. B. (2008). Significance of the composition profiles associated with dunite bodies in the Josephine and Trinity ophiolites. *Geochemistry, Geophysics, Geosystems* doi:10.1029/2008GC001954.

Nermond, S. (1994). *Etude expérimentale de la recristallisation statique et de la cinétique de croissance de l'olivine*. Université de Paris 7, 204 pp.

Nowicki, T., Crawford, B., Dyck, D., Carlson, J. A., McElroy, R., Oshust, P. A. & Helmstaedt, H. (2004). The geology of kimberlite pipes of the Ekati property, NWT, Canada. *Lithos* **76**, 1–27.

Nowicki, T., Porritt, L., Crawford, B. & Kjarsgaard, B. (2008). Geochemical trends in kimberlites of the Ekati property, Northwest Territories, Canada: Insights on volcanic and resedimentation processes. *Journal of Volcanology and Geothermal Research* **174**, 117–127.

Peslier, A. H., Woodland, A. B. & Wolff, J. A. (2008). Fast kimberlite ascent rates estimated from hydrogen diffusion profiles in xenolithic mantle olivines from southern Africa. *Geochimica et Cosmochimica Acta* **72**, 2711–2722.

Poirier, J. P. & Nicolas, A. (1975). Deformation induced recrystallization due to progressive misorientation of subgrains, with special reference to mantle peridotites. *Journal of Geology* **83**, 707–720.

Price, S. E., Russell, J. K. & Kopylova, M. G. (2000). Primitive magma from the Jericho Pipe, N.W.T., Canada: Constraints on primary kimberlite melt chemistry. *Journal of Petrology* **41**, 789–808.

Raleigh, C. B. & Kirby, S. H. (1970). *Creep in the upper mantle*. Mineralogical Society of America Special Paper 3, pp. 113–121.

Scott-Smith, B. H. S. (1992). Kimberlites and lamproites. *Exploration Mining Geology* **1**, 371–381.

Shaw, C. S. J., Thibault, Y., Edgar, A. D. & Lloyd, F. E. (1998). Mechanisms of orthopyroxene dissolution in silica undersaturated melts at 1 atmosphere and implications for the origin of silica-rich glass in mantle xenoliths. *Contributions to Mineralogy and Petrology* **132**, 354–370.

Shirey, S. B., Harris, J. W., Richardson, S. R., Fouch, M. J., James, D. E., Cartigny, P., Deines, P. & Viljoen, F. (2002). Diamond genesis, seismic structure and evolution of the Kaapvaal–Zimbabwe craton. *Science* **297**, 1683–1686.

Simon, N. S. C., Carlson, R. W., Pearson, D. G. & Davies, G. R. (2007). The origin and evolution of the Kaapvaal cratonic lithospheric mantle. *Journal of Petrology* **48**, 589–625.

Smith, C. B., Gurney, J. J., Skinner, E. M. W., Clement, C. R. & Ebrahim, N. (1985). Geochemical character of southern African kimberlites: a new approach based on isotopic constraints. *Transactions of the Geological Society of South Africa* **88**, 267–280.

Sobolev, A. V., Hofmann, A. W., Kuzmin, D. V. *et al*. (2007). Estimating the amount of recycled crust in sources of mantle-derived melts. *Science* **316**, 412–417.

Stachel, T., Harris, J. W., Tappert, R. & Brey, G. P. (2003). Peridotitic inclusions in diamonds from the Slave and the Kaapvaal cratons—similarities and differences based on a preliminary data set. *Lithos* **71**, 489–503.

Van der Wal, D., Chopra, P. N., Drury, M. R. & Fitz Gerald, J. (1993). Relationships between dynamically recrystallized grain size and deformation conditions in experimentally deformed olivine rocks. *Geophysical Research Letters* **20**, 1479–1482.

Walter, M. J. (1999). Melting residues of fertile peridotite and the origin on cratonic lithosphere. In: Fei, Y., Bertka, C. M. & Mysen, B. O. (eds) *Mantle Petrology: Field Observations and High-pressure Experimentation*. Houston, TX: Geochemical Society, pp. 225–240.

Wilson, L. & Head, J. W., III (2007). An integrated model of kimberlite ascent and eruption. *Nature* **447**, 53–57.

Wyllie, P. J. (1980). The origin of kimberlite. *Journal of Geophysical Research* **85**, 6902–6910.